Phenomenology of a single right-handed neutrino seesaw model

Mariana Henriques de Araújo

Thesis to obtain the Master of Science Degree in

Engineering Physics

Supervisor: Prof. Dr. Filipe Rafael Joaquim

Examination Committee

Chairperson: Prof. Dr. Maria Teresa Haderer de la Peña Stadler
Supervisor: Prof. Dr. Filipe Rafael Joaquim
Member of the Committee: Prof. Dr. Ricardo Jorge Gonzalez Felipe

September 2017

Acknowledgments

I would like to thank my supervisor, Prof. Dr. Filipe Joaquim, for his support over the entire process of constructing this thesis. His dedication, availability and involvement made the experience much more pleasant and enlightening than it might have been otherwise and I consider myself lucky to have had him as a supervisor.

I would also like to thank my family: my brother, who has already been through this experience and shared useful advice and support, and my parents, who know nothing about particle physics and were patient enough to listen to my fascinated monologues on neutrino physics.

Finally, I want to thank my friends in MEFT, Mariana, Martim and Rita, who shared my worries and joys over these five years, and those two closest to me, without whom I could not imagine doing this: my favorite cat, Zelda, and my favorite person, Madalena.

Resumo

O Modelo Padrão é notavelmente bem sucedido na descrição das interações de partículas elementares. No entanto, a observação experimental de oscilações de neutrinos impõe a necessidade de estender o modelo de alguma forma, para acomodar massas e mistura de neutrinos.

Nesta tese, consideramos uma extensão em particular, restrita por uma simetria A_4, com um neutrino de direita num singleto de A_4 e três dubletos de Higgs num tripleto de A_4. As massas dos neutrinos surgem devido a um mecanismo de *seesaw*, e o sector de neutrinos resultante é estudado a baixas energias, através de um processo numérico que gera pontos aleatoriamente no espaço de parâmetros do potencial escalar de Higgs, de modo a aplicar as equações do grupo de renormalização. A análise é repetida com a inclusão de um termo no potencial de Higgs que quebra A_4 suavemente.

Verificamos que os valores experimentais para as diferenças de massas quadradas e ângulos de mistura dos neutrinos só são reproduzidos no caso de quebra suave de A_4.

Keywords: Modelo Padrão, Massas e mistura de neutrinos, Simetria A_4, Mecanismo de *see-saw*

Abstract

The Standard Model is remarkably successful at describing the interactions of elementary particles. However, the experimental observation of neutrino oscillation imposes the necessity of extending the model in some way to accommodate for neutrino masses and mixing.

In this thesis, we consider a particular extension, constrained by an A_4 symmetry, with one right-handed neutrino in an A_4 singlet and three Higgs doublets in an A_4 triplet. Neutrino masses arise due to a seesaw mechanism, and the resulting neutrino sector is studied at low energy, through a numerical process which generates points randomly in the parameter space of the Higgs scalar potential in order to apply renormalization group equations. The analysis is repeated with the inclusion of a term in the Higgs potential which breaks A_4 softly.

We find that experimental measurements of neutrino mass-squared differences and mixing angles are only reproduced in the case of soft breaking of A_4.

Keywords: Standard Model, Neutrino masses and mixing, A_4 symmetry, Seesaw mechanism

Contents

List of Tables

List of Figures

List of Abbreviations

CC	Charged Current
CKM	Cabibbo-Kobayashi-Maskawa
EWSB	Electroweak Symmetry Breaking
LH	Left-Handed
NC	Neutral Current
PMNS	Pontecorvo-Maki-Nakagawa-Sakata
RGE	Renormalization Group Equations
RH	Right-Handed
SM	Standard Model
SSB	Spontaneous Symmetry Breaking
VEV	Vacuum Expectation Value

Chapter 1

Introduction

Particle physics is remarkably well described by the Standard Model (SM), which relates elementary matter particles, both quarks and leptons, with three of the four fundamental forces: the strong, the weak and the electromagnetic forces. The SM is a gauge quantum field theory, with the first step towards its construction being given by Glashow [1], who discovered, in 1961, a way to combine the electromagnetic and weak interactions into a single electroweak model ruled by an SU(2)$\times$U(1) symmetry. Quarks and their interactions with the strong force were described by an SU(3) symmetry in what is called the Eightfold Way, formulated in 1964 [2, 3] and later absorbed as a component of the SM, so that its formulation came to be based on an SU(3)$\times$SU(2)$\times$U(1) symmetry. In 1967, the SM was defined in its current form [4, 5] with the incorporation of the Higgs mechanism [6, 7, 8], which introduces a new field, the Higgs field, that gives rise to the masses of all elementary particles through the mechanism of spontaneous symmetry breaking (SSB).

Several experimental observations were made, which were overwhelmingly in agreement with the predictions of the SM. Some examples are the discovery of neutral weak currents, caused by Z boson exchange, in 1973 [9, 10, 11], the discovery of the $W^{\pm}$ [12, 13] and Z [14, 15] bosons themselves in 1983, and the recent discovery of the Higgs boson, in 2012 [16, 17]. These and dozens of other experimental observations contribute to the acknowledgment of the SM as a theory that is incredibly successful in describing the interactions of elementary particles. However, there are some areas of elementary particle physics which the SM cannot fully describe. One of these pertains to neutrinos.

1.1 A brief history of neutrinos

Neutrinos are very light electrically neutral leptons that exist in three generations, associated with the three generations of charged leptons: electron, muon and tau neutrinos. The existence of neutrinos was first postulated by Pauli in 1930, in order to explain the phenomenon of beta decay, in which a nucleus N^0 emits a proton p^+, with the observable emission of an electron e^-. If the interaction were indeed given by

$$N^0 \rightarrow p^+ + e^- \,, \tag{1.1}$$

then it would be a two-body decay and the resulting particles would have a fixed energy. Instead, the energy spectrum for the electron was found to be continuous [18]. Pauli's proposed solution to this problem was that a third undetected particle was being produced in the decay: a light, electrically neutral particle which he named neutron. With the discovery of the neutron as we know it, which is a neutral particle n^0 of similar mass to the proton, this nomenclature was abandoned. It was Fermi who took up the problem, naming the light particle neutrino and suggesting, in 1934 [19], that beta decay was a three-body decay of the form

$$n^0 \to p^+ + e^- + \overline{\nu_e}\,, \tag{1.2}$$

where $\overline{\nu_e}$ is the electron anti-neutrino. Due to the form of the electron energy spectrums, it was determined that the neutrino should either be massless or have a very small mass. It is established in the SM that neutrinos are massless.

Because neutrinos are electrically neutral leptons, they don't interact through the electromagnetic or strong forces, making direct detection difficult. It was only in 1956 that the existence of neutrinos was confirmed, in the Cowan-Reines experiment [20]. Anti-neutrinos produced by beta decay reacted with protons through

$$\overline{\nu_e} + p^+ \to n^0 + e^+\,, \tag{1.3}$$

and the resulting positron e^+ quickly annihilated itself with an electron, producing detectable radiation, while the neutron was captured by an an appropriate nucleus, also producing radiation. The coincidence of both emissions was the unique signature of the electron anti-neutrino interaction. The two remaining types of neutrino were detected later, the muon neutrino in 1962 [21] and the tau neutrino in 2000 [22].

In the late 1960s, the Homestake experiment was established to detect neutrinos emitted by nuclear fusion in the Sun, which interacted with a large deposit of perchloroethylene through

$$\nu_e + {}^{37}\mathrm{Cl} \to {}^{37}\mathrm{Ar} + e^-\,. \tag{1.4}$$

The amount of Argon collected in the deposit would correspond to the amount of iteractions that had ocurred, so that it would be possible to determine the amount of neutrinos that had interacted. The results of the experiment were held in disbelief, as it was found that only one third of the predicted interactions were taking place [23], in what was called the solar neutrino problem. It was widely admitted that a mistake had been made, either in the theoretical prediction or in the experimental observations, but both were scrutinized closely with no errors found. Later experiments for the detection of neutrinos corroborated the results of the Homestake experiment.

Many ideas were suggested to explain the difference between theory and experiment, including the hypothesis of neutrino oscillation. This phenomenon was first predicted by Pontecorvo in 1957 [24]. He postulated that if neutrinos had a very small but nonzero mass, then it was possible that their mass states, in which they had definite mass, did not correspond to their flavor states, in which they interacted through the weak force, but rather to a quantum superposition of those states. Then neutrinos, which were produced in definite flavor states, would propagate through space as a superposition of mass

states, with each of the mass states acquiring a different quantum phase, which in turn would cause the neutrinos to become a superposition of flavor states as well. When neutrinos reached detectors and interacted, there was a possibility that each of the flavor states in the superposition would interact. In this way, electron neutrinos produced in the Sun could travel to the Earth and there interact as muon or tau neutrinos, due to neutrino oscillation. In the end, neutrino oscillation was confirmed by the SNO experiment, which used heavy water as a neutrino detector, making it capable of detecting two reactions, one which involved only electron neutrinos, and one which was sensitive to all three neutrino flavors. The experimental results were that the flux of neutrinos from the Sun was in agreement with the theory, but only one third of those neutrinos were interacting as electron neutrinos [25].

The confirmation of neutrino oscillation did solve the solar neutrino problem, but in doing so required the existence of nonzero neutrino masses, which contradict the formulation of the SM. Thus, we find that neutrino phenomenology is not fully described by the SM and it is necessary to alter it in a way that accommodates for neutrino masses and oscillation. This is a rich topic of study in current times, with many different extensions of the SM being suggested. This thesis will focus on one such model.

1.2 Objectives and outline

As stated above, the purpose of this thesis is to study an extension of the SM in which neutrino masses arise. We specify the fields and constraints being added to the SM and study the resulting terms in the Lagrangian of the theory. Based on these terms, we obtain expressions for the parameters of the neutrino sector related to neutrino mass and neutrino oscillation and compare them with the experimental results available. Finally, we conclude as to the validity of the proposed model, depending on whether we can determine conditions for which the model is in agreement with experimental data.

This thesis is organized as follows. In Chapter 2, we present an overview of the SM formulation, focusing on the electroweak sector. We move on to Chapter 3, where we address the problem of neutrino mass and some ways in which the SM can be extended to include massive neutrinos. In Chapter 4, we introduce our model, with extensions in both the fermionic and scalar sectors and a new imposed symmetry. We study the resulting neutrino masses at a very high energy scale and at the scale of current experiments and conclude upon the validity of the model. In Chapter 5, we softly break the imposed symmetry and study the effects on the neutrino masses and remaining parameters of the neutrino sector, concluding upon the validity of the model in this case. Finally, in Chapter 6 we present our conclusions and suggest further work to be done on the topic. Additional calculations related to the minimization of the Higgs potential for our model are presented in Appendix A, at the end of the thesis.

Chapter 2

The Standard Model of particle physics

The SM is based on the gauge group SU(3)$_c$×SU(2)$_L$×U(1)$_Y$. Here c stands for color, L for left-handedness and Y for hypercharge. The matter content of the SM is [26]:

$$\text{Fermions}\begin{cases}\textbf{Quarks} & q_{L\alpha} \equiv \begin{pmatrix} u_{L\alpha} \\ d_{L\alpha} \end{pmatrix} \sim (3,2,1/6)\,, \\ & u_{R\alpha} \sim (3,1,2/3)\ ,\ d_{R\alpha} \sim (3,1,-1/3)\,, \\ \textbf{Leptons} & \ell_{L\alpha} \equiv \begin{pmatrix} \nu_{L\alpha} \\ l_{L\alpha} \end{pmatrix} \sim (1,2,-1/2)\,, \\ & l_{R\alpha} \sim (1,1,-1)\,, \end{cases} \qquad (2.1)$$

$$\textbf{Higgs}\ \phi \equiv \begin{pmatrix} \phi^+ \\ \phi^0 \end{pmatrix} \sim (1,2,1/2)\,,$$

where the numbers in brackets indicate how the fields transform under the SM gauge group. The first number describes how the field transforms under SU(3)$_c$ (1 for a singlet, 3 for a triplet) and the second how it transforms under SU(2)$_L$ (1 for a singlet, 2 for a doublet). The third number is the hypercharge Y of the field, given by

$$Y = Q - T_3\,, \qquad (2.2)$$

where Q is the electric charge and T_3 is the third component of weak isospin. The fields u_α and d_α correspond to up- and down-type quarks, and ν_α and l_α to neutrinos and charged leptons, respectively. The index α runs through the three generations of fermions, while the subscripts L and R denote the chirality of the field, which can be left-handed (LH) or right-handed (RH), respectively. Chirality is defined by a field transformation law under application of the operator $\gamma^5 = i\gamma^0\gamma^1\gamma^2\gamma^3$, where γ^μ are the Dirac

matrices forming a Clifford Algebra. Namely,

$$\gamma^5\psi_R = \psi_R \quad , \quad \gamma^5\psi_L = -\psi_L \, . \tag{2.3}$$

Any field can be decomposed into its RH and LH components, $\psi = \psi_R + \psi_L = P_R\psi + P_L\psi$, by the application of the projection operators $P_{R,L}$:

$$P_{R,L} = \frac{1 \pm \gamma^5}{2} \, . \tag{2.4}$$

We focus on the electroweak sector of the SM, corresponding to the group SU(2)$_L$×U(1)$_Y$. The electroweak Lagrangian density (identified as the Lagrangian in the following) is

$$\begin{aligned} \mathcal{L}_{\text{SM}} =& (D^\mu\phi)^\dagger(D_\mu\phi) - V(\phi) - \frac{1}{4}W^a_{\mu\nu}W^{a\mu\nu} - \frac{1}{4}B_{\mu\nu}B^{\mu\nu} \\ &+ i\overline{\ell_{L\alpha}}\not{D}\ell_{L\alpha} + i\overline{q_{L\alpha}}\not{D}q_{L\alpha} + i\overline{l_{R\alpha}}\not{D}l_{R\alpha} + i\overline{u_{R\alpha}}\not{D}u_{R\alpha} + i\overline{d_{R\alpha}}\not{D}d_{R\alpha} \\ &- (\mathbf{Y}^l_{\alpha\beta}\overline{\ell_{L\alpha}}\phi l_{R\beta} + \text{H.c.}) - (\mathbf{Y}^u_{\alpha\beta}\overline{q_{L\alpha}}\tilde{\phi}u_{R\beta} + \text{H.c.}) - (\mathbf{Y}^d_{\alpha\beta}\overline{q_{L\alpha}}\phi d_{R\beta} + \text{H.c.}) \, . \end{aligned} \tag{2.5}$$

In this equation, the Feynman slash notation, $\not{p} = \gamma^\mu p_\mu$, is used, as well as the definitions $\overline{\psi} \equiv \psi^\dagger\gamma^0$ and $\tilde{\phi} \equiv i\tau_2\phi^*$. $\mathbf{Y}^l$, $\mathbf{Y}^u$ and $\mathbf{Y}^d$ are general 3×3 complex Yukawa matrices and H.c. denotes the Hermitian conjugate. Local gauge invariance requires replacing the ordinary derivative ∂_μ by a covariant derivative D_μ given by

$$D_\mu \equiv \partial_\mu - igW^a_\mu\frac{\tau_a}{2} - ig'B_\mu Y \, . \tag{2.6}$$

Y stands for the generator of U(1)$_Y$ and τ^a $(a = 1, 2, 3)$ are the Pauli matrices (generators of SU(2)$_L$). The vector fields B_μ and W^a_μ $(a = 1, 2, 3)$ are introduced to ensure local U(1)$_Y$ and SU(2)$_L$ gauge invariance, respectively. The number of vector fields required to ensure local gauge invariance under the action of a group is equal to the number of generators of that group. Thus, there are three W_μ fields and one B_μ field. The corresponding invariant kinetic terms are constructed using the field strengths

$$B_{\mu\nu} \equiv \partial_\mu B_\nu - \partial_\nu B_\mu \quad , \quad W^a_{\mu\nu} \equiv \partial_\mu W^a_\nu - \partial_\nu W^a_\mu - g\epsilon^{abc}W^b_\mu W^c_\nu \, . \tag{2.7}$$

As for the potential associated to the scalar field ϕ, one has the most general $V(\phi)$, invariant under the SU(2)$_L$×U(1)$_Y$ gauge group:

$$V(\phi) = \mu^2\phi^\dagger\phi + \lambda(\phi^\dagger\phi)^2 \, , \tag{2.8}$$

where μ has dimensions of mass and λ is a dimensionless parameter. One can notice that there are no mass terms in the Lagrangian of (2.5), as no such term would be invariant under the gauge group. This is obvious for gauge fields. For fermions, a mass term would be of the form $-m\overline{\psi}\psi = -m(\overline{\psi_L}\psi_R + \overline{\psi_R}\psi_L)$, which would imply combining an SU(2)$_L$ doublet with an SU(2)$_L$ singlet, thus leading to a term that is not invariant under SU(2)$_L$. Focusing on the hypercharge of such a term, we have for the RH field $Y = Q$ and for the LH field $Y = Q - T_3$. Thus, we obtain a hypercharge of T_3 for $\overline{\psi_L}\psi_R$ and $-T_3$ for $\overline{\psi_R}\psi_L$, concluding that the mass term is not invariant under U(1)$_Y$. There seems to be a mass term for the

scalar Higgs field in the potential of (2.8), but this is contingent on having $\mu^2 > 0$, which, as we will see, is not interesting from the theoretical viewpoint.

This incongruence, given that elementary particles are known to be massive, is lifted by the Higgs mechanism. After SSB in the electroweak sector, mass terms arise for bosons and fermions. The former obtain mass from the Higgs kinetic term, the latter from the Yukawa terms, the last line in (2.5).

2.1 The Higgs mechanism

SSB occurs when the Lagrangian of a theory respects a certain symmetry but the vacuum state (or lowest energy state) does not. In the case of the SM, the vacuum is identified as the configuration of the field ϕ which minimizes (2.8). For $\mu^2 > 0$, the minimization condition is $|\phi| = 0$, while for $\mu^2 < 0$, it is $|\phi|^2 \equiv |v_{\text{SM}}|^2 = -\mu^2/2\lambda$. Thus, in this case, the fields possess a nonzero value in the vacuum. If a charged field has a nonzero vacuum expectation value (VEV), then the vacuum has an electric charge, which cannot occur as electric charge is a conserved quantity of the SM. Since only neutral fields can acquire a nonzero value in the vacuum, we have

$$\langle\phi\rangle = \begin{pmatrix} \langle\phi^+\rangle \\ \langle\phi^0\rangle \end{pmatrix} = \begin{pmatrix} 0 \\ v_{\text{SM}} \end{pmatrix} . \tag{2.9}$$

In general, the minimization condition sets $v_{\text{SM}} = e^{i\theta}\sqrt{-\frac{\mu^2}{2\lambda}}$. Choosing a particular VEV corresponds to fixing a value for θ. We fix $\theta = 0$, thus realizing electroweak symmetry breaking (EWSB). The Higgs field can be parametrized as oscillations around the vacuum state as

$$\phi(x) = \exp\left(i\frac{\xi^a(x)\tau^a}{\sqrt{2}v_{\text{SM}}}\right)\begin{pmatrix} 0 \\ v_{\text{SM}} + \frac{H(x)}{\sqrt{2}} \end{pmatrix} . \tag{2.10}$$

Here, $H(x)$ and $\xi(x)$ are real fields with zero VEV, so that (2.9) is valid. Before SSB, it is possible to apply a gauge transformation to ϕ, leaving the Lagrangian invariant. By choosing the unitary gauge, we can absorb the exponential and obtain

$$\phi(x) = \begin{pmatrix} 0 \\ v_{\text{SM}} + \frac{H(x)}{\sqrt{2}} \end{pmatrix} . \tag{2.11}$$

After EWSB, $H(x)$ will correspond to the physical Higgs boson field. Replacing (2.11) in the Lagrangian of (2.5), the VEV v_{SM} gives rise to new terms. Starting with the scalar and gauge sectors, we obtain

$$D_\mu\phi = \begin{pmatrix} 0 \\ \frac{\partial_\mu H}{\sqrt{2}} \end{pmatrix} - i\frac{g}{2}\begin{pmatrix} W_\mu^1 - iW_\mu^2 \\ -W_\mu^3 \end{pmatrix}(v_{\text{SM}} + H/\sqrt{2}) - i\frac{g'}{2}\begin{pmatrix} 0 \\ B_\mu \end{pmatrix}(v_{\text{SM}} + H/\sqrt{2}) , \tag{2.12}$$

$$V(\phi) = \frac{\lambda}{4}H^4 + \sqrt{2}\lambda v_{\text{SM}}H^3 - \mu^2H^2 + \text{const.} . \tag{2.13}$$

Defining the field combinations

$$\begin{aligned} W_\mu^+ &= (W_\mu^-)^\dagger = \frac{1}{\sqrt{2}}(W_\mu^1 - iW_\mu^2)\,, \\ A_\mu &= \sin\theta_W W_\mu^3 + \cos\theta_W B_\mu\,, \\ Z_\mu &= \cos\theta_W W_\mu^3 - \sin\theta_W B_\mu\,, \end{aligned} \tag{2.14}$$

where θ_W is the so-called weak mixing angle, one obtains the following bilinear terms in the scalar and gauge fields:

$$(D^\mu\phi)^\dagger(D_\mu\phi) - V(\phi) = \frac{1}{2}(-2\mu^2)H^2 + \frac{g^2 v_{\mathsf{SM}}^2}{2} W^{\mu-}W_\mu^+ + \frac{1}{2}\frac{g^2 v_{\mathsf{SM}}^2}{2\cos^2\theta_W} Z^\mu Z_\mu + \dots\,. \tag{2.15}$$

Thus, upon EWSB, the Higgs (H) and gauge ($W^\pm, Z$) bosons obtain masses

$$m_H = \sqrt{-2\mu^2} = 2v_{\mathsf{SM}}\sqrt{\lambda} \quad , \quad m_W = \frac{g v_{\mathsf{SM}}}{\sqrt{2}} \quad , \quad m_Z = \frac{g v_{\mathsf{SM}}}{\sqrt{2}\cos\theta_W} = \frac{m_W}{\cos\theta_W}\,. \tag{2.16}$$

The remaining field A_μ is massless, and is identified as being the photon.

2.2 Lepton electroweak currents

Before analyzing how EWSB grants mass to fermions, we study the lepton-gauge boson interaction terms in (2.5):

$$\begin{aligned} \mathcal{L}^l_{\mathsf{Gauge}} =& i\overline{\ell_{L\alpha}}\left(-ig\not{W}^a\frac{\tau^a}{2} + ig'\not{B}\frac{1}{2}\right)\ell_{L\alpha} + i\overline{l_{R\alpha}}\left(0 + ig'\not{B}\right)l_{R\alpha} \\ =& \frac{1}{2}\overline{\ell_{L\alpha}}\begin{pmatrix} (gs_W - g'c_W)\not{A} + (gc_W + g's_W)\not{Z} & \sqrt{2}g\not{W}^+ \\ \sqrt{2}g\not{W}^- & -(gs_W + g'c_W)\not{A} - (gc_W - g's_W)\not{Z} \end{pmatrix}\ell_{L\alpha} \\ & - g'\overline{l_{R\alpha}}(c_W\not{A} - s_W\not{Z})l_{R\alpha}\,. \end{aligned} \tag{2.17}$$

We have used the fields of (2.14), together with the simplified notation $s_W \equiv \sin\theta_W$ and $c_W \equiv \cos\theta_W$. The diagonal interaction terms, combining particles with the same electric charge, correspond to the neutral-current (NC) Lagrangian $\mathcal{L}_{\mathsf{NC}}$, while the off-diagonal ones describe charged currents (CC) $\mathcal{L}_{\mathsf{CC}}$. Namely,

$$\begin{aligned} \mathcal{L}^\ell_{\mathsf{NC}} =& \frac{1}{2}\overline{\nu_{L\alpha}}\left[(gs_W - g'c_W)\not{A} + (gc_W + g's_W)\not{Z}\right]\nu_{L\alpha} \\ & - \frac{1}{2}\overline{l_{L\alpha}}\left[(gs_W + g'c_W)\not{A} + (gc_W - g's_W)\not{Z}\right]l_{L\alpha} - g'\overline{l_{R\alpha}}\left(c_W\not{A} - s_W\not{Z}\right)l_{R\alpha}\,, \end{aligned} \tag{2.18}$$

$$\mathcal{L}^\ell_{\mathsf{CC}} = \frac{g}{\sqrt{2}}\left(\overline{\nu_{L\alpha}}\not{W}^+ l_{L\alpha} + \overline{l_{L\alpha}}\not{W}^-\nu_{L\alpha}\right)\,. \tag{2.19}$$

By requiring that neutrinos do not couple with the photon, the condition $(gs_W - g'c_W) = 0$ is obtained, yielding $\tan\theta_W = g'/g$. Therefore,

$$\mathcal{L}_Z^\ell = \frac{g}{c_W}\left(\frac{1}{2}\overline{\nu_{L\alpha}}\gamma^\mu\nu_{L\alpha} - \frac{1}{2}(c_W^2 - s_W^2)\overline{l_{L\alpha}}\gamma^\mu l_{L\alpha} + s_W^2\overline{l_{R\alpha}}\gamma^\mu l_{R\alpha}\right)Z_\mu\,. \tag{2.20}$$

$$\begin{aligned}\mathcal{L}_A^\ell =& -\frac{1}{2}2g'c_W\overline{l_{L\alpha}}\not{A}l_{L\alpha} - g'c_W\overline{l_{R\alpha}}\not{A}l_{R\alpha} \\ =& -g'c_W(\overline{l_{L\alpha}}\not{A}l_{L\alpha} + \overline{l_{R\alpha}}\not{A}l_{R\alpha}) = -g'c_W\bar{l}\gamma^\mu l A_\mu\,,\end{aligned} \tag{2.21}$$

The Lagrangians $\mathcal{L}_{\text{NC}}$ and $\mathcal{L}_{\text{CC}}$ describe the interactions between leptons and the physical gauge bosons.

2.3 Fermion masses

After EWSB, the Yukawa terms in the Lagrangian read

$$-\mathcal{L}_{\text{Yuk.}} = \left(v_{\text{SM}} + \frac{H}{\sqrt{2}}\right)\left(\mathbf{Y}^l_{\alpha\beta}\overline{l_{L\alpha}}l_{R\beta} + \mathbf{Y}^u_{\alpha\beta}\overline{u_{L\alpha}}u_{R\beta} + \mathbf{Y}^d_{\alpha\beta}\overline{d_{L\alpha}}d_{R\beta} + \text{H.c.}\right)\,. \tag{2.22}$$

Considering only the bilinear terms in the fermion fields, and defining the mass matrices for the ψ fields $\mathbf{M}^\psi = v_{\text{SM}}\mathbf{Y}^\psi$, we obtain

$$-\mathcal{L}_{\text{Yuk.}} = (\mathbf{M}^l_{\alpha\beta}\overline{l_{L\alpha}}l_{R\beta} + \mathbf{M}^u_{\alpha\beta}\overline{u_{L\alpha}}u_{R\beta} + \mathbf{M}^d_{\alpha\beta}\overline{d_{L\alpha}}d_{R\beta} + \text{H.c.}) + \dots\,, \tag{2.23}$$

where the missing terms describe fermion-Higgs interactions. In general, the fermion mass terms formed in this way are not diagonal, meaning that they mix different generations. In order to bring these fields to the physical basis, where the mass matrices are diagonal, we must perform a "rotation" in flavor space. The bi-diagonalization of the matrices $\mathbf{M}$ is performed by unitary matrices $V^{l,u,d}_{L,R}$:

$$\begin{aligned}V_L^{l^\dagger}\mathbf{M}^l V_R^l &= \text{diag}(m_e, m_\mu, m_\tau) \equiv \mathbf{D}^l\,, \\ V_L^{u^\dagger}\mathbf{M}^u V_R^u &= \text{diag}(m_u, m_c, m_t) \equiv \mathbf{D}^u\,, \\ V_L^{d^\dagger}\mathbf{M}^d V_R^d &= \text{diag}(m_d, m_s, m_b) \equiv \mathbf{D}^d\,.\end{aligned} \tag{2.24}$$

From the relations above, we conclude that we can change to a basis where the fermion fields are mass eigenstates by performing the rotations

$$\begin{aligned}l_L \to V_L^l l_L\ ,\ l_R \to V_R^l l_R\,, \\ u_L \to V_L^u u_L\ ,\ u_R \to V_R^u u_R\,, \\ d_L \to V_L^d d_L\ ,\ d_R \to V_R^d d_R\,.\end{aligned} \tag{2.25}$$

These transformations operate differently on the two components of the SU(2)$_L$ doublet $q_{L\alpha}$. Considering the quark-gauge interaction terms, which are analogous to those of (2.17), we see that the NC term

is unaffected by this rotation, while the CC term becomes

$$\mathcal{L}^q_{\text{CC}} = \frac{g}{\sqrt{2}} \overline{u_L} V_L^{u\dagger} \gamma^\mu V_L^d d_L W^+_\mu + \text{H.c.}\,. \tag{2.26}$$

This defines the quark mixing matrix, or Cabibbo-Kobayashi-Maskawa (CKM) matrix [27, 28], $V_{\text{CKM}} \equiv V_L^{u\dagger} V_L^d$. An interpretation of the presence of the quark mixing matrix in the CC interaction is that massive up-type quarks do not interact with the massive down-type quarks of their generation individually, but rather with combinations of down-type quarks defined by the rotation $V_{\text{CKM}} d_L$.

As V_{CKM} is a unitary matrix of dimension $n \times n$, where n is the number of generations, it can be described by n^2 parameters, of which $n(n-1)/2$ are moduli that correspond to mixing angles. The remaining parameters are $n(n+1)/2$ complex phases. Not all of these phases are physical since the Lagrangian, aside from the CC terms, is invariant under the transformations

$$u_{L,R\alpha} \to e^{i\varphi^u_\alpha} u_{L,R\alpha} \;\;,\;\; d_{L,R\alpha} \to e^{i\varphi^d_\alpha} d_{L,R\alpha}. \tag{2.27}$$

Thus, by applying such rephasings to quarks, we expect to remove up to $2n$ phases from the mixing matrix. However, these transformations would correspond to a global rotation of all quarks followed by a rephasing with $2n-1$ distinct phases. Therefore, only $2n-1$ phases in V_{CKM} are unphysical. For the case of $n = 3$, there are three mixing angles θ_{12}, θ_{13}, θ_{23}, and one phase δ. The mixing matrix is commonly parametrized [29] as

$$V_{\text{CKM}} = \begin{pmatrix} c_{12}c_{13} & s_{12}c_{13} & s_{13}e^{-i\delta} \\ -s_{12}c_{23} - c_{12}s_{23}s_{13}e^{i\delta} & c_{12}c_{23} - s_{12}s_{23}s_{13}e^{i\delta} & s_{23}c_{13} \\ s_{12}s_{23} - c_{12}c_{23}s_{13}e^{i\delta} & -c_{12}s_{23} - s_{12}c_{23}s_{13}e^{i\delta} & c_{23}c_{13} \end{pmatrix}, \tag{2.28}$$

where $s_{ij} \equiv \sin\theta_{ij}$ and $c_{ij} \equiv \cos\theta_{ij}$.

In the case of leptons, due to the absence of RH neutrino fields in the SM, there is no term in $\mathcal{L}_{SM}$ leading to a Dirac neutrino mass term upon EWSB. Thus, **neutrinos are massless in the SM**. This means that performing a rotation of the neutrino fields such as the ones in (2.25) will not affect the diagonalization of any mass matrix. Then we can define the transformation

$$\nu_L \to V_L^l \nu_L\,, \tag{2.29}$$

which ensures that both the NC and the CC terms remain unchanged by the diagonalization of the charged-lepton mass matrix. Consequently, no lepton mixing matrix arises.

Chapter 3

Neutrino masses and mixing

As shown in the previous chapter, neutrinos are massless in the SM due to the absence of RH neutrino fields. This is motivated by the experimental observation that neutrinos produced in weak interactions are always LH [30]. However, experimental results of neutrino oscillation have revealed that neutrinos have mass, with three distinct mass-squared differences, indicating that at least two massive neutrinos exist [31]. Thus, extensions of the SM must be considered in order to account for neutrino masses.

3.1 Effective neutrino masses and lepton mixing

Neutrino mass terms can be accounted for in the SM by adding sterile RH neutrinos ν_R, which are SU(2)$_L$ singlets with null hypercharge, meaning that they do not interact with the gauge fields. Upon this addition, Yukawa terms like those of (2.5) can be constructed, leading to neutrino mass matrices of the form $\mathbf{M}^\nu = v_{\text{SM}}\mathbf{Y}^\nu$. Although neutrino masses have not been determined experimentally, an upper limit of 2 eV has been determined from tritium decay experiments [32]. This is several orders of magnitude below the mass of the lightest charged fermion, the electron. Thus, the Yukawa terms for neutrinos would have to be much smaller than those of the remaining leptons in order to generate these small neutrino masses. There is a mass difference of a few orders of magnitude between the lightest and heaviest of charged fermions, but the difference between the electron and neutrino masses is even larger. This seems to suggest a distinct mechanism for neutrino mass generation, one which could account for such a deviation from the pattern followed by the charged fermions. One way to justify such a distinct mass for neutrinos would be to introduce a neutrino Majorana mass term [33].

Since neutrinos are neutral fermions, they can be defined as their own antiparticles,

$$\nu = \nu^C \,, \tag{3.1}$$

where the antiparticle of a fermion ψ is defined as $\psi^C \equiv C\overline{\psi}^T$. C is the charge conjugation matrix, which obeys $C{\gamma^\mu}^T C^{-1} = -\gamma^\mu$. The property (3.1) characterizes a Majorana particle. No charged fermion can be a Majorana particle, as particles and antiparticles have opposite charge. Given $\gamma^5 \equiv i\gamma^0\gamma^1\gamma^2\gamma^3$, we

can conclude

$$\gamma^5(\psi_L)^C = (\psi_L)^C\,, \tag{3.2}$$

which determines that the antiparticle of a LH field is a RH field. This leads to a new mass term for the LH neutrinos of the SM, called the Majorana mass term, defined as

$$-\frac{1}{2}m\overline{\nu_L}\nu_L^C + \text{H.c.}\,. \tag{3.3}$$

There are some complications involving this mass term in the SM. The first is that such a term will break any U(1) symmetry under which ν_L is charged, due to the fact that neutrino fields can no longer be rephased at will. Since $\nu = \nu^C$, the rephasing must be the same for ν and for ν^C, which is inconsistent with the definition of ν^C as an antiparticle. In the SM, the broken symmetry is lepton number L, and the Majorana mass term generates transitions $\Delta L = 2$.

The second complication is more severe: LH neutrinos are part of an SU(2)$_L$ doublet. As such, there must be additional fields in the mass term in order to form an invariant of the gauge group. Given the field content of the SM, there is no way to form such an invariant that is also renormalizable. Waiving the requirement of renormalization, the lowest dimensional term which induces Majorana mass terms under EWSB is the five-dimensional Weinberg operator [34],

$$\mathcal{L}_{\text{Wein.}} = c_{\alpha\beta}\frac{1}{\Lambda}\left(\overline{\ell_{L\alpha}^C}\tilde{\phi}^*\right)\left(\tilde{\phi}^\dagger\ell_{L\beta}\right) + \text{H.c.}\,, \tag{3.4}$$

where the $c_{\alpha\beta}$ are complex coefficients. The presence of a non-renormalizable term such as the Weinberg operator in the effective Lagrangian suggests that the SM is not a complete theory, but rather one valid at low energies. We would expect that the exact theory manifests itself only at energies of the order of a high-energy scale Λ, considered in (3.4) as an energy cutoff. Upon EWSB, the Weinberg operator becomes

$$\mathcal{L}_{\text{Wein.}} = \frac{v_{\text{SM}}^2}{\Lambda}\left(c_{\alpha\beta}\overline{\nu_{L\alpha}^C}\nu_{L\beta} + \text{H.c.}\right) + \mathcal{L}_{\text{int.}}^{H\nu}\,, \tag{3.5}$$

where $\mathcal{L}_{\text{int.}}^{H\nu}$ contains neutrino-Higgs interaction terms. Thus, comparison with (3.3) yields the Majorana mass matrix

$$\mathbf{M}_{\alpha\beta}^{\nu} = -\frac{2v_{\text{SM}}^2}{\Lambda}c_{\alpha\beta}\,. \tag{3.6}$$

The presence of a neutrino mass matrix, as in the case of quarks, will lead to mixing between lepton generations in electroweak currents upon diagonalization. Because the Majorana mass matrix is symmetric, it can be diagonalized by a single unitary transformation, V_L^ν. As such, in addition to the charged-lepton transformations of (2.25), we define

$$\nu_{L\alpha} \to (V_L^\nu)_{\alpha i}\nu_{Li}\,, \tag{3.7}$$

where the fields ν_i have definite masses m_i. The CC term of (2.19) becomes, under this transformation,

$$\mathcal{L}_{\text{CC}}^{\ell} = \frac{g}{\sqrt{2}}\left[\overline{\nu_{Li}}\gamma^\mu(V_L^{\nu^\dagger}V_L^l)_{i\alpha}l_{L\alpha}W_\mu^+ + \text{H.c.}\right]\,. \tag{3.8}$$

Parameter	Best fit $\pm 1\sigma$ (3σ range)	
	Normal	Inverted
$\frac{\Delta m^2_{21}}{10^{-5}\,\text{eV}^2}$	$7.50^{+0.19}_{-0.17}$ $(7.03 \to 8.09)$	
$\frac{\Delta m^2_{3\ell}}{10^{-3}\,\text{eV}^2}$	$+2.524^{+0.039}_{-0.040}$ $(+2.407 \to +2.643)$	$-2.514^{+0.038}_{-0.041}$ $(-2.635 \to -2.399)$
$\sin^2\theta_{12}$	$0.306^{+0.012}_{-0.012}$ $(0.271 \to 0.345)$	
$\sin^2\theta_{23}$	$0.441^{+0.027}_{-0.021}$ $(0.385 \to 0.635)$	$0.587^{+0.020}_{-0.024}$ $(0.393 \to 0.640)$
$\frac{\sin^2\theta_{13}}{100}$	$2.166^{+0.075}_{-0.075}$ $(1.934 \to 2.392)$	$2.179^{+0.076}_{-0.076}$ $(1.953 \to 2.408)$
$\delta/^\circ$	261^{+51}_{-59} $(0 \to 360)$	277^{+40}_{-46} $(145 \to 391)$

Table 3.1: Best-fit values and 3σ allowed ranges of the three-neutrino oscillation parameters in the NO and IO cases, obtained from a global fit of current neutrino oscillation data [31]. Note that $\Delta m^2_{3\ell} \equiv \Delta m^2_{31} > 0$ ($\Delta m^2_{3\ell} \equiv \Delta m^2_{32} < 0$) for NO (IO).

The lepton mixing matrix, known as the Pontecorvo-Maki-Nakagawa-Sakata (PMNS) matrix [35, 36], is thus defined by

$$U_{\text{PMNS}} \equiv V_L^{l\dagger} V_L^{\nu} \,. \tag{3.9}$$

As aforementioned, the neutrino fields cannot be rephased due to their Majorana nature. This means that, whereas we could remove up to $2n-1$ phases from the CKM matrix, in this case only n phases can be removed. For $n=3$ generations, the PMNS matrix is then parametrized by three mixing angles and three phases. Namely [32],

$$U_{\text{PMNS}} = \begin{pmatrix} c_{12}c_{13} & s_{12}c_{13} & s_{13}e^{-i\delta} \\ -s_{12}c_{23} - c_{12}s_{23}s_{13}e^{i\delta} & c_{12}c_{23} - s_{12}s_{23}s_{13}e^{i\delta} & s_{23}c_{13} \\ s_{12}s_{23} - c_{12}c_{23}s_{13}e^{i\delta} & -c_{12}s_{23} - s_{12}c_{23}s_{13}e^{i\delta} & c_{23}c_{13} \end{pmatrix} \begin{pmatrix} e^{-i\alpha_1/2} & 0 & 0 \\ 0 & e^{-i\alpha_2/2} & 0 \\ 0 & 0 & 1 \end{pmatrix} , \tag{3.10}$$

where $s_{ij} \equiv \sin\theta_{ij}$ and $c_{ij} \equiv \cos\theta_{ij}$. θ_{ij} are the lepton mixing angles, δ is a Dirac-type phase and $\alpha_{1,2}$ are Majorana phases, arising due to the Majorana character of neutrinos. We conclude that the low-energy neutrino sector of the (effective) SM Lagrangian contains nine parameters: three mixing angles, three phases and three neutrino masses.

Neutrinos are produced and detected in definite flavor states, but they evolve in time according to the values of their masses. Since neutrino flavor states are superpositions of mass eigenstates with distinct masses, neutrinos may oscillate between different flavors. A determination of the oscillation probability, such as that in [33], concludes that it is not dependent on the neutrino masses m_i, but rather on the mass-squared differences $\Delta m^2_{ij} = m^2_i - m^2_j$. As the sign of Δm^2_{31} is indeterminate (while Δm^2_{21} is positive), there are two possible orderings of neutrino masses, normal ordering (NO) or inverted ordering (IO), corresponding to

$$\text{NO: } m_1 < m_2 < m_3 \quad , \quad \text{IO: } m_3 < m_1 < m_2 \,. \tag{3.11}$$

Current global fits to all presently available oscillation data by Esteban *et al.* [31] are summarized in Table 3.1. Other analyses are those of Capozzi *et al.* [37], and Forero *et al.* [38].

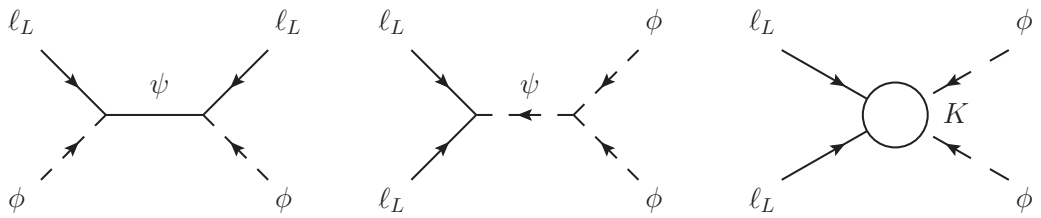

Figure 3.1: Tree-level interactions mediated by new heavy particles, in type I and III seesaw mechanisms (left) and type II seesaw mechanisms (center), which give rise to the Weinberg operator of (3.4) at low energies (right). Notice that $K \propto c/\Lambda$ [see (3.4)].

3.2 The seesaw mechanism

If the SM is an effective theory, then the complete theory which describes particle physics must have additional degrees of freedom, described by fields that are decoupled at low energy. As such, these fields must have large masses, comparable to the scale Λ in (3.4). Extensions of the SM using the seesaw mechanism consider a tree-level interaction between lepton and Higgs fields mediated by new heavy particles. At low energy, this interaction reduces to a four-point vertex of the form $\ell\ell\phi\phi$, such as that of (3.4). Upon EWSB, this term will generate neutrino Majorana masses. For the seesaw mechanism to be possible, the extra fields ψ can be added in two ways. Type I [39, 40, 41, 42, 43] and III [44] seesaw mechanisms consider fields with interaction terms $\psi\phi\ell$ (left diagram in Figure 3.1), while the type II [45, 46, 47, 48, 48] seesaw mechanism considers fields with $\psi\ell\ell$ and $\psi\phi\phi$ terms (center diagram in Figure 3.1).

Focusing on the $\psi\phi\ell$ interaction terms, the condition of gauge invariance, given the representation assignments of ϕ and ℓ_L, imposes that ψ must have null hypercharge and must transform as either an SU(2)$_L$ singlet (type I seesaw) or triplet (type III seesaw). We reach the latter conclusion by obtaining the Kronecker product of SU(2) representations $\mathbf{2} \otimes \mathbf{2} = \mathbf{1} \oplus \mathbf{3}$ and observing that $\mathbf{3} \otimes \mathbf{3}$ contains the trivial representation. The fields ψ must be fermionic due to angular momentum conservation.

We consider the type I seesaw mechanism in particular. In this case, the fields ψ are singlets of zero hypercharge. Thus, n_R sterile RH neutrinos ν_{Ri} are added to the SM. Using these fields, we can form a neutrino Yukawa term which gives rise to Dirac masses upon EWSB. We can also define a Majorana mass term for the RH neutrinos. The Lagrangian for this extended theory will therefore be

$$\mathcal{L}_{\text{I}} = \mathcal{L}_{\text{SM}} + \frac{i}{2}\left[\overline{\nu_R}\gamma^\mu\partial_\mu\nu_R - \overline{\nu_R}\gamma^\mu\overleftarrow{\partial_\mu}\nu_R\right] - \left[\mathbf{Y}^\nu_{\alpha i}\overline{\ell^0_{L\alpha}}\tilde{\phi}\nu_{Ri} + \frac{1}{2}(\mathbf{M}_R)_{ij}\overline{\nu^C_{Ri}}\nu_{Rj} + \text{H.c.}\right], \tag{3.12}$$

where the first term in brackets is the kinetic term for right-handed neutrinos, ℓ^0_L denotes the left-handed lepton fields in the weak basis, as opposed to the mass basis, and $\mathbf{M}_R$ is the Majorana mass matrix. Because the Majorana mass term is a singlet of SU(2)$_L$ with zero hypercharge, and thus invariant under the action of the gauge symmetries of the theory, the value of $\mathbf{M}_R$ is not protected by these gauge

symmetries and is free to be arbitrarily large. After EWSB, the neutrino terms in (3.12) are

$$\begin{aligned}\mathcal{L}_{\mathsf{I}}^{\nu} =& \frac{g}{2c_W}\overline{\nu_L^0}\gamma^\mu Z_\mu \nu_L^0 + \frac{g}{\sqrt{2}}\left[\overline{l_{L\alpha}^0}\gamma^\mu W_\mu^- \nu_{L\alpha}^0 + \text{H.c.}\right] \\ &+ \left[\frac{i}{2}\overline{\nu_L^0}\gamma^\mu\partial_\mu\nu_L^0 + \frac{i}{2}\overline{\nu_R}\gamma^\mu\partial_\mu\nu_R - (\mathbf{m}_D)_{\alpha i}\overline{\nu_{L\alpha}^0}\nu_{Ri} - \frac{1}{2}(\mathbf{M}_R)_{ij}\overline{\nu_{Ri}^C}\nu_{Rj} + \text{H.c.}\right] \\ =& \frac{g}{2c_W}\overline{n_L^0}\gamma^\mu Z_\mu \mathbf{d}_{\mathsf{NC}}^{\nu} n_L^0 + \left[\frac{g}{\sqrt{2}}\overline{l_L^0}\gamma^\mu W_\mu^- \mathbf{d}_{\mathsf{CC}} n_L^0 + \frac{i}{2}\overline{n_L^0}\gamma^\mu\partial_\mu n_L^0 - \frac{1}{2}\overline{n_L^0}\mathcal{M}(n_L^0)^C + \text{H.c.}\right].\end{aligned} \tag{3.13}$$

In the last equation we can find, in order of appearance, the NC and CC terms, the kinetic terms and the mass terms. $\mathbf{m}_D$ is the $3 \times n_R$ Dirac mass matrix and $\mathbf{M}_R$ is the $n_R \times n_R$ Majorana mass matrix. We use the definitions

$$\begin{aligned} n_L^0 &\equiv \begin{pmatrix}\nu_L^0 \\ \nu_R^C\end{pmatrix} \ , \ \mathcal{M} = \begin{pmatrix}\mathbf{0} & \mathbf{m}_D \\ \mathbf{m}_D^T & \mathbf{M}_R\end{pmatrix}, \\ \mathbf{d}_{\mathsf{NC}}^{\nu} &= \begin{pmatrix}\mathbf{1}_{3\times 3} & \mathbf{0} \\ \mathbf{0} & \mathbf{0}\end{pmatrix} \ , \ \mathbf{d}_{\mathsf{CC}} = \begin{pmatrix}\mathbf{1}_{3\times 3} & \mathbf{0}\end{pmatrix}. \end{aligned} \tag{3.14}$$

Since the mass matrix $\mathcal{M}$ is symmetric, it can be diagonalized through a unitary transformation

$$\mathbf{U}^\dagger \mathcal{M} \mathbf{U}^* = \mathbf{d}_{n_L} \ , \ \mathbf{d}_{n_L} = \begin{pmatrix}\mathbf{d}_\nu & \mathbf{0} \\ \mathbf{0} & \mathbf{d}_M\end{pmatrix}, \tag{3.15}$$

with $\mathbf{d}_\nu \equiv \text{diag}(m_1, m_2, m_3)$ and $\mathbf{d}_M \equiv \text{diag}(M_1, \ldots, M_{n_R})$, which will correspond to the masses of the three light components and the n_R heavy components, respectively, in the limit $\mathbf{M}_R \gg \mathbf{m}_D$. The mass eigenstates are defined as

$$n_L^0 = \mathbf{U} n_L \equiv \begin{pmatrix}\mathbf{V} & \mathbf{S} \\ \mathbf{R} & \mathbf{T}\end{pmatrix}\begin{pmatrix}\nu_{lL} \\ \nu_{hL}\end{pmatrix}, \tag{3.16}$$

where the matrix $\mathbf{U}$ has been written in block form. Using this form of $\mathbf{U}$ and (3.15), we obtain the system of equations

$$\mathbf{U}^\dagger \mathcal{M} = \mathbf{d}_{n_L}\mathbf{U}^T \Leftrightarrow \begin{cases}\mathbf{R}^\dagger \mathbf{m}_D^T = \mathbf{d}_\nu \mathbf{V}^T \\ \mathbf{T}^\dagger \mathbf{m}_D^T = \mathbf{d}_M \mathbf{S}^T \\ \mathbf{S}^\dagger \mathbf{m}_D + \mathbf{T}^\dagger \mathbf{M}_R = \mathbf{d}_M \mathbf{T}^T \\ \mathbf{V}^\dagger \mathbf{m}_D + \mathbf{R}^\dagger \mathbf{M}_R = \mathbf{d}_\nu \mathbf{R}^T\end{cases}, \tag{3.17}$$

which, for $\mathbf{M}_R \gg \mathbf{m}_D$, allows us to determine

$$\mathbf{R} \simeq -(\mathbf{M}_R^*)^{-1}\mathbf{m}_D^\dagger \mathbf{V} + \mathcal{O}\left(\frac{v_{\mathsf{SM}}^3}{M^3}\right) \Rightarrow \mathbf{d}_\nu \mathbf{V}^T \simeq -\mathbf{V}^\dagger \mathbf{m}_D \mathbf{M}_R^{-1}\mathbf{m}_D^T. \tag{3.18}$$

From the unitarity of $\mathbf{U}$, we obtain $\mathbf{V}^\dagger\mathbf{V} = \mathbf{1} - \mathbf{R}^\dagger\mathbf{R}$. Therefore, we arrive at

$$\mathbf{d}_\nu \simeq -\mathbf{V}^\dagger \mathbf{m}_D \mathbf{M}_R^{-1}\mathbf{m}_D^T \mathbf{V}^* + \mathcal{O}\left(\frac{v_{\mathsf{SM}}^4}{M^3}\right). \tag{3.19}$$

The Lagrangian with only the light fields is given by

$$\begin{aligned}\mathcal{L}_\nu^{\text{light}} =& \frac{g}{2c_W}\overline{\nu_{lL}}\gamma^\mu Z_\mu \mathbf{V}^\dagger \mathbf{V}\nu_{lL} + \frac{g}{\sqrt{2}}\left[\overline{l_L^0}\gamma^\mu W_\mu^- \mathbf{V}\nu_{lL} + \text{H.c.}\right] \\ &+ \left[\frac{i}{2}\overline{\nu_{lL}}\gamma^\mu\partial_\mu\nu_{lL} - \frac{1}{2}\overline{\nu_{lL}}\left(-\mathbf{V}^\dagger\mathbf{m}_D\mathbf{M}_R^{-1}\mathbf{m}_D^T\mathbf{V}^*\right)\nu_{lL}^C + \text{H.c.}\right].\end{aligned} \tag{3.20}$$

Up to $\mathcal{O}\left(v_{\text{SM}}^2/M^2\right)$, the matrix $\mathbf{V}$ is unitary and thus we can rotate the light mass eigenstates ν_{lL} by $\mathbf{V}^{-1}$ without adding flavor-changing neutral currents or off-diagonal elements in the kinetic term. We obtain, in this basis, the light-neutrino mass matrix

$$\mathbf{m}_\nu \simeq -\mathbf{m}_D\mathbf{M}_R^{-1}\mathbf{m}_D^T\,. \tag{3.21}$$

The same procedure can be followed in the heavy neutrino sector, with Lagrangian

$$\begin{aligned}\mathcal{L}_\nu^{\text{heavy}} =& \frac{g}{2c_W}\overline{\nu_{hL}}\mathbf{S}^\dagger\mathbf{S}\gamma^\mu Z_\mu\nu_{hL} + \frac{g}{\sqrt{2}}\left[\overline{l_L^0}\gamma^\mu W_\mu^-\mathbf{S}\nu_{hL} + \text{H.c.}\right] \\ &+ \left[\frac{i}{2}\overline{\nu_{hL}}\gamma^\mu\partial_\mu\nu_{hL} - \frac{1}{2}\overline{\nu_{hL}}\mathbf{d}_M\nu_{hL}^C + \text{H.c.}\right].\end{aligned} \tag{3.22}$$

Using (3.17), we determine

$$\mathbf{d}_M \simeq \mathbf{T}^\dagger\left[\mathbf{M}_R + (\mathbf{M}_R^*)^{-1}\mathbf{m}_D^\dagger\mathbf{m}_D + \mathbf{m}_D^T\mathbf{m}_D^*(\mathbf{M}_R^*)^{-1}\right]\mathbf{T}^*\,, \tag{3.23}$$

and, given $\mathbf{S}^\dagger\mathbf{S} = \mathbf{1} - \mathbf{T}^\dagger\mathbf{T}$, we parametrize the perturbations to the unitarity of $\mathbf{T}$ as

$$\mathbf{T} \simeq \left(\mathbf{1} - \frac{1}{2}(\mathbf{M}_R^*)^{-1}\mathbf{m}_D^\dagger\mathbf{m}_D\mathbf{M}_R^{-1}\right)\mathbf{K}_h + \mathcal{O}\left(\frac{v_{\text{SM}}^4}{M^4}\right)\,, \tag{3.24}$$

where $\mathbf{K}_h$ is a unitary matrix. The transformation $\nu_{hL}^0 = \mathbf{K}_h\nu_{hL}$ ensures that the kinetic term has no off-diagonal elements. In the end, we obtain the heavy-neutrino effective mass matrix

$$\mathbf{M}_{\text{eff}} \simeq \mathbf{M}_R + \frac{1}{2}\left[(\mathbf{M}_R^*)^{-1}\mathbf{m}_D^\dagger\mathbf{m}_D + \mathbf{m}_D^T\mathbf{m}_D^*(\mathbf{M}_R^*)^{-1}\right]\,. \tag{3.25}$$

With three generations of RH neutrinos ($n_R = 3$), the mass matrix $\mathbf{m}_\nu$ has, in general, three distinct nonzero eigenvalues. We can count the parameters of the neutrino sector in this SM extension, going to the basis where $\mathbf{M}_R$ is diagonal. Since $\mathbf{m}_D$ is a 3×3 complex matrix, it has eighteen parameters, of which three can be removed by rephasing. There are also three heavy Majorana masses, for a total of eighteen parameters. Given that, at low energies, the neutrino sector is described by only nine parameters, we conclude that the full theory cannot be reconstructed using only low-energy neutrino data. In the case $n_R = 2$, it is also possible to obtain three distinct mass-squared differences, although one of the neutrinos is massless. The number of parameters is reduced to eleven, still larger than the seven parameters at low energies (two neutrino masses, three mixing angles and two complex phases). With a single RH neutrino, the seesaw mechanism is no longer viable, as the effective neutrino mass matrix has two zero eigenvalues.

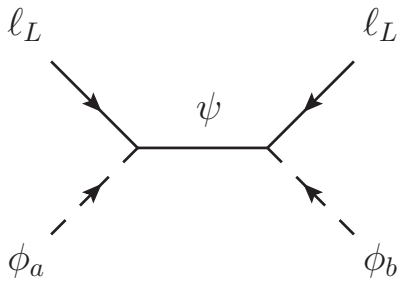

Figure 3.2: Tree-level interaction mediated by new heavy particles, in the type I seesaw mechanism, for a model with multiple Higgs doublets ϕ_i with $i = 1, 2, \ldots, n_H$.

3.3 Type I seesaw with more than one Higgs doublet

So far, the discussion of SM extensions has been focused on expanding the fermion sector of the SM. However, extensions of the scalar sector, in which additional Higgs doublets are considered, are also viable. In a theory with n_H Higgs doublets, the scalar potential takes the general form [49]

$$V(\phi) = \text{quadratic terms} + \lambda_{ijkl}\left(\phi_i^\dagger \phi_j\right)\left(\phi_k^\dagger \phi_l\right) , \tag{3.26}$$

where the λ_{ijkl} are dimensionless couplings which satisfy $\lambda_{ijkl} = \lambda_{klij} = \lambda^*_{jilk}$. The indices i, j, k, l run over the n_H doublets. The lepton Yukawa Lagrangian becomes

$$-\mathcal{L}^{\ell}_{\text{Yuk.}} = (Y_i^l)_{\alpha\beta}\overline{\ell_{L\alpha}}\phi_i l_{R\beta} + \text{H.c.}\,, \tag{3.27}$$

giving mass to the charged leptons upon SSB. The five-dimensional Weinberg operator is generalized to n_H^2 operators $\mathcal{O}_{ij}$, which take the form

$$\mathcal{O}_{ij} = \left(\overline{\ell^C_{L\alpha a}}\kappa^{ij}_{\alpha\beta}\ell_{L\beta c}\right)(\varepsilon^{ab}\phi_{ib})(\varepsilon^{cd}\phi_{jd})\,, \tag{3.28}$$

where the indices a, b, c, d are SU(2)$_L$ indices that distinguish between the two components of SU(2)$_L$ doublets, and ϵ is the antisymmetric tensor with $\varepsilon^{12} = 1$. The κ^{ij} are flavor coupling matrices with dimension -1 which satisfy $\kappa^{ij} = \kappa^{ji^T}$. We consider the implementation of the type I seesaw mechanism with n_H Higgs doublets and determine the form of κ^{ij} in this case.

With n_H Higgs doublets ϕ_i, the interactions represented in the left diagram of Figure 3.1 take the form presented in Figure 3.2. The changes with respect to the $n_H = 1$ case are reflected in the Lagrangian of the extended theory, which varies from (3.12) in the Yukawa term. Namely,

$$\mathcal{L}_{\text{I}} = \mathcal{L}_{\text{SM}} + \frac{i}{2}\left[\overline{\nu_R}\gamma^\mu\partial_\mu\nu_R - \overline{\nu_R}\gamma^\mu\overleftarrow{\partial_\mu}\nu_R\right] - \left[(\mathbf{Y}^\nu_{\alpha i})_a\,\overline{\ell^0_{L\alpha}}\tilde{\phi}_a\nu_{Ri} + \frac{1}{2}(\mathbf{M}_R)_{ij}\overline{\nu^C_{Ri}}\nu_{Rj} + \text{H.c.}\right] , \tag{3.29}$$

where $a = 1, 2, \ldots, n_H$. Recalling the calculations of the previous section, we obtain the light-neutrino

mass matrix $\mathbf{m}_\nu$ given by (3.21), applying the redefinition

$$\mathbf{m}_D = v_{\text{SM}} \mathbf{Y}^\nu \to v_a \mathbf{Y}^\nu_a \,, \tag{3.30}$$

where $\langle \phi^0_a \rangle = v_a$ is the VEV of the neutral component of the Higgs doublet ϕ_a. Thus, the effective neutrino mass matrix in the case of n_H Higgs doublets is

$$\mathbf{m}_\nu \simeq - \sum_{a,b=1}^{n_H} v_a v_b \mathbf{Y}^\nu_a \mathbf{M}_R^{-1} \mathbf{Y}_b^{\nu^T} \,. \tag{3.31}$$

Comparing this expression with the generalized mass operators $\mathcal{O}_{ij}$ of (3.28), we determine

$$\kappa^{ab} = \mathbf{Y}^\nu_a \mathbf{M}_R^{-1} \mathbf{Y}_b^{\nu^T} \,. \tag{3.32}$$

To conclude, in the case of $n_H > 1$ there is more than one effective neutrino mass operator contributing to $\mathbf{m}_\nu$. In the next chapter we will focus on the phenomenology of a specific model with $n_H = 3$, $n_R = 1$ and an imposed A_4 discrete symmetry.

Chapter 4

Single right-handed neutrino A_4 model

In the previous chapter, we discussed extensions of the SM which can account for neutrino mass generation. When implemented, these extensions will, in general, lead to a significant increase in the number of free parameters. In order to reduce this excessive freedom and obtain a more predictive model, the typical prescription is to introduce new symmetries which the theory must obey, enforcing relations between parameters. Recently, discrete flavor symmetries have been the focus of interest in the literature [50]. Our model considers one such symmetry, given by the A_4 group, which is a popular choice within discrete symmetries.

The popularity of the A_4 group is not arbitrary. As will be shown in Section 4.1, all fields under A_4 must be assigned to either a singlet or a triplet. Given that there are three generations of fermions in the SM, this is the ideal set of representations for an extension of the SM that adds particles in sets of three. The most common option is to add three RH neutrinos in a triplet, thus enlarging the fermionic sector and obtaining the results mentioned in Section 3.2, namely three nonzero neutrino masses. In our model, we consider instead the minimal fermionic extension, consisting of a single RH neutrino, and enlarge the scalar sector in order to have three Higgs doublets. It has been shown in the previous chapter that adding a single RH neutrino to the SM cannot lead to three distinct neutrino mass-squared differences through the type I seesaw mechanism. However, when simultaneously expanding the scalar sector, the conclusions regarding the single RH neutrino scenario may not apply. Thus, in this chapter, we explore an A_4 model with one RH neutrino assigned to an A_4 singlet and three Higgs doublets transforming as a triplet of the same group.

4.1 The A_4 group

A_4 is a subgroup of the group of permutations of four elements S_4 which contains the even permutations. It has twelve elements partitioned into four conjugacy classes:

$$\begin{aligned} C_1 &= \{e\}\,, & C_3 &= \{(123),(142),(134),(243)\}\,, \\ C_2 &= \{(12)(34),(13)(24),(14)(23)\}\,, & C_4 &= \{(132),(124),(143),(234)\}\,. \end{aligned} \tag{4.1}$$

	χ_1	χ_2	χ_3	χ_4
$\mathbf{1}$	1	1	1	1
$\mathbf{1}'$	1	1	ω	ω^2
$\mathbf{1}''$	1	1	ω^2	ω
$\mathbf{3}$	3	-1	0	0

Table 4.1: Character table for the group A_4. We take $\omega = \exp(i2\pi/3)$.

The number of irreducible representations (irreps) of the group is equal to the number of conjugacy classes [51]. Of these, the 1D irreps will be those of the group $\mathsf{A}_4/[\mathsf{A}_4, \mathsf{A}_4]$. Since the commutator $[\mathsf{A}_4, \mathsf{A}_4]$ is isomorphic to the Klein group $\mathcal{K} = \mathbb{Z}_2 \times \mathbb{Z}_2$, of order 4, we have $\#\mathsf{A}_4/[\mathsf{A}_4, \mathsf{A}_4] = 12/4 = 3$ and therefore there are three 1D irreps of A_4. We determine that the final irrep has dimension 3 by the relation

$$\sum_\mu n_\mu^2 = n_G \,, \tag{4.2}$$

where the sum is over all inequivalent irreps, n_μ is the dimension of the irrep μ and n_G is the order of the group. The character table for the group can be constructed from the known 1D irreps of $\mathbb{Z}_3$ (the only group of order 3) and the relations of orthogonality and orthonormality

$$\sum_\mu \frac{n_i}{n_G} (\chi_i^\mu)^* \chi_j^\mu = \delta^{ij} \;\;,\;\; \sum_i \frac{n_i}{n_G} (\chi_i^\mu)^* \chi_i^\nu = \delta^{\mu\nu} \,, \tag{4.3}$$

where n_i is the number of elements in a class and $\chi_i^\mu \equiv \mathrm{Tr}\,[\mathbf{U}^\mu(g)]$ is the character of an element $g \in C_i$ in the irrep μ. We obtain the character table given in Table 4.1.

Any element in the group can be obtained from the two generators, $\mathfrak{s} \equiv (12)(34)$ and $\mathfrak{t} \equiv (123)$. For example, $(134) = \mathfrak{ts}$. Thus, the definition of $\mathbf{U}^\mu(\mathfrak{s})$ and $\mathbf{U}^\mu(\mathfrak{t})$ defines a basis for a representation μ. A group representation R can be decomposed as a direct sum of irreducible representations of the group,

$$\mathbf{U}^R(g) = \bigoplus_\mu a_\mu \mathbf{U}^\mu(g) \,, \tag{4.4}$$

where a_μ is the multiplicity of the irrep μ, which can be determined using

$$a_\mu = (\tilde{\chi}^\mu)^\dagger \cdot \tilde{\chi}^R \;\;,\;\; \tilde{\chi}_i^R = \sqrt{\frac{n_i}{n_G}} \chi_i^R \,. \tag{4.5}$$

We can apply this equation to the Kronecker product of irreps and obtain its direct sum decomposition, taking into account $\chi_i^{\mu\times\nu} = \chi_i^\mu \times \chi_i^\nu$. The results are

$$\begin{aligned}
\mathbf{1} \otimes \mathbf{1} &= \mathbf{1}' \otimes \mathbf{1}'' = \mathbf{1} \,, \\
\mathbf{1} \otimes \mathbf{1}' &= \mathbf{1}'' \otimes \mathbf{1}'' = \mathbf{1}' \,, \\
\mathbf{1} \otimes \mathbf{1}'' &= \mathbf{1}' \otimes \mathbf{1}' = \mathbf{1}'' \,, \\
\mathbf{1} \otimes \mathbf{3} &= \mathbf{1}' \otimes \mathbf{3} = \mathbf{1}'' \otimes \mathbf{3} = \mathbf{3} \,, \\
\mathbf{3} \otimes \mathbf{3} &= \mathbf{1} \oplus \mathbf{1}' \oplus \mathbf{1}'' \oplus \mathbf{3} \oplus \mathbf{3} \,.
\end{aligned} \tag{4.6}$$

The exact form of the invariants obtained by the tensor product of two A_4 triplets will depend on the choice of basis for the 3D irrep. For the Ma-Rajasekaran basis, the product $(a_1, a_2, a_3) \otimes (b_1, b_2, b_3)$ leads to the invariants [52]

$$\begin{aligned} &a_1b_1 + a_2b_2 + a_3b_3 \sim \mathbf{1}\,, \\ &a_1b_1 + \omega^2 a_2b_2 + \omega a_3b_3 \sim \mathbf{1'}\,, \\ &a_1b_1 + \omega a_2b_2 + \omega^2 a_3b_3 \sim \mathbf{1''}\,, \end{aligned} \qquad \begin{pmatrix} a_2b_3 \\ a_3b_1 \\ a_1b_2 \end{pmatrix} \sim \mathbf{3_1}\,, \qquad \begin{pmatrix} a_3b_2 \\ a_1b_3 \\ a_2b_1 \end{pmatrix} \sim \mathbf{3_2}\,. \tag{4.7}$$

The $\mathbf{1}$ components of the tensor product $\mathbf{3} \otimes \mathbf{3} \otimes \mathbf{3}$, which will be used further ahead, are given by

$$\left[\begin{pmatrix} a_1 \\ a_2 \\ a_3 \end{pmatrix} \otimes \begin{pmatrix} b_1 \\ b_2 \\ b_3 \end{pmatrix} \otimes \begin{pmatrix} c_1 \\ c_2 \\ c_3 \end{pmatrix} \right]_{\mathbf{1}} = (a_2b_3c_1 + a_3b_1c_2 + a_1b_2c_3) \oplus (a_3b_2c_1 + a_1b_3c_2 + a_2b_1c_3)\ . \tag{4.8}$$

4.2 A_4 scalar potential

As discussed in Section 3.3, when n_H increases, the scalar potential takes a more complex form, with a larger number of free parameters. In the case of three Higgs doublets placed in a triplet representation of A_4, i.e., $\Phi = (\phi_1, \phi_2, \phi_3) \sim \mathbf{3}$, the A_4-invariant potential is given by [53]

$$\begin{aligned} V(\Phi) =& m^2 \sum_i \phi_i^\dagger \phi_i + \frac{1}{2}\lambda_1 \left(\sum_i \phi_i^\dagger \phi_i \right)^2 + \lambda_2 \left(\phi_1^\dagger \phi_1 + \omega^2 \phi_2^\dagger \phi_2 + \omega \phi_3^\dagger \phi_3 \right) \left(\phi_1^\dagger \phi_1 + \omega \phi_2^\dagger \phi_2 + \omega^2 \phi_3^\dagger \phi_3 \right) \\ &+ \lambda_3 \left[\left(\phi_2^\dagger \phi_3 \right) \left(\phi_3^\dagger \phi_2 \right) + \left(\phi_3^\dagger \phi_1 \right) \left(\phi_1^\dagger \phi_3 \right) + \left(\phi_1^\dagger \phi_2 \right) \left(\phi_2^\dagger \phi_1 \right) \right] \\ &+ \left\{ \frac{1}{2}\lambda_4' \left[\left(\phi_2^\dagger \phi_3 \right)^2 + \left(\phi_3^\dagger \phi_1 \right)^2 + \left(\phi_1^\dagger \phi_2 \right)^2 \right] + \text{H.c.} \right\}\ . \end{aligned} \tag{4.9}$$

The parameters m, λ_1, λ_2, λ_3 are real. The parameter λ_4' is complex and its phase can be made evident by the redefinition $\lambda_4' = \lambda_4 e^{i\alpha}$, where λ_4 and α are real. This potential is determined to have global minima for four distinct VEV configurations, valid in different regions of the parameter space. These are [54]

$$\begin{aligned} h_1 &= v(1,0,0)\,, & h_2 &= v(1,1,1)\,, \\ h_3 &= v(\pm 1, \eta, \eta^*)\,, & h_4 &= v(1, e^{i\alpha_4}, 0)\,, \end{aligned} \tag{4.10}$$

where $\eta = \exp(i\pi/3)$ and $v, \alpha_4 \in \Re$. The parameter v can be related to v_{SM}, defined in Section 2.1. Take, for example, the boson masses given in (2.16). From the expressions for these masses in a model with three Higgs doublets, which must return the known values of m_W and m_Z, we obtain the condition

$$|v_1|^2 + |v_2|^2 + |v_3|^2 = v_{\text{SM}}^2\,, \tag{4.11}$$

which fixes the normalization v. In order to determine the dimensionless couplings λ_{ijkl}, $V(\Phi)$ can be defined in the form of (3.26). The results will be presented in Section 4.6 (Table 4.2).

The neutrino mass matrix can be determined using (3.31), as the addition of a heavy RH neutrino

implements a type I seesaw mechanism. In this case, the Majorana mass matrix reduces to the Majorana mass of the single RH neutrino, M_R. The 3×1 Dirac mass matrix $\mathbf{m}_D$ is obtained, after SSB, from a Yukawa term such as the one in (3.29),

$$-Y_\alpha^{\nu i}\overline{\ell_{L\alpha}}\tilde{\phi}_i\nu_R + \text{H.c.}. \xrightarrow{\text{SSB}} \mathbf{m}_D = v_i\mathbf{Y}^{\nu i}\,. \tag{4.12}$$

The product of fields must be performed according to the representation assignment of each field and the multiplication rules of A_4, given by (4.7), so that we guarantee the invariance of the Yukawa term under A_4.

Before studying the neutrino mass matrix, a related issue must first be tackled. With the representation assignments of the RH neutrino and of the Higgs doublets fixed by the model, it is necessary to determine the assignments for the LH lepton doublets ℓ_L, so that the field product of (4.12) can be determined. This can be done by studying the charged-lepton mass matrix, which also yields the assignments of the RH charged leptons l_R [55].

4.3 Charged-lepton masses

The charged-lepton mass matrix can be obtained through SSB from the Yukawa term given in (3.27), with the condition that the field product must be invariant under A_4. We wish to find the representation assignments for ℓ_L and l_R which lead to three distinct nonzero eigenvalues of the charged-lepton mass matrix, corresponding to the well-known values of m_e, m_μ and m_τ.

There are four possibilities for assignments, determined by whether the three ℓ_L and l_R are assigned to a triplet or to three singlets. The case where both are assigned to singlets is immediately discarded, as it can be seen from (4.6) that $\mathbf{1}, \mathbf{1}', \mathbf{1}'' \otimes \mathbf{3} \otimes \mathbf{1}, \mathbf{1}', \mathbf{1}'' = \mathbf{3}$ regardless of which singlet representation is used, and the Higgs doublets are assigned to a triplet of A_4. Thus, it is not possible in this case to obtain a charged-lepton Yukawa term that is invariant under A_4. This leaves three possibilities.

4.3.1 ℓ_L triplet, l_R triplet

In this case, the field product $\overline{\ell_L}\Phi l_R$ is of the form $\mathbf{3} \otimes \mathbf{3} \otimes \mathbf{3}$. The $\mathbf{1}$ components of this tensor product are given by (4.8). Thus, the Yukawa term takes the form

$$\begin{aligned} &-y_1(\overline{\mu_L}\phi_3 e_R + \overline{\tau_L}\phi_1\mu_R + \overline{e_L}\phi_2\tau_R) - y_2(\overline{\tau_L}\phi_2 e_R + \overline{e_L}\phi_3\mu_R + \overline{\mu_L}\phi_1\tau_R) + \text{H.c.} \\ &\xrightarrow{\text{SSB}} -(\overline{e_L} \quad \overline{\mu_L} \quad \overline{\tau_L}) \begin{pmatrix} 0 & y_2v_3 & y_1v_2 \\ y_1v_3 & 0 & y_2v_1 \\ y_2v_2 & y_1v_1 & 0 \end{pmatrix} \begin{pmatrix} e_R \\ \mu_R \\ \tau_R \end{pmatrix} + \text{H.c.}\,, \end{aligned} \tag{4.13}$$

where we consider the general VEV (v_1, v_2, v_3). The charged-lepton masses are the square roots of the eigenvalues of the matrix $\mathbf{M}^l\mathbf{M}^{l^\dagger}$, with characteristic polynomial

$$\lambda^3 - \lambda^2 \left(y_1^2 + y_2^2\right) \left(|v_1|^2 + |v_2|^2 + |v_3|^2\right) + \lambda \left[y_1^2 y_2^2 \left(|v_1|^4 + |v_2|^4 + |v_3|^4\right) + \left(y_1^4 + y_2^4\right) \left(|v_1 v_2|^2 + |v_2 v_3|^2 + |v_1 v_3|^2\right)\right] - \left(y_1^3 + y_2^3\right)^2 |v_1 v_2 v_3|^2 \,. \tag{4.14}$$

We replace the general VEVs v_i with those given by the configurations h_i defined in (4.10). For the vacuum configurations h_1 and h_4, one of the eigenvalues is clearly zero. For h_2 and h_3, we obtain

$$m_1^e = m_2^e = v\sqrt{y_1^2 + y_2^2 - y_1 y_2} \;\;,\;\; m_3^e = v\,|y_1 + y_2| \;. \tag{4.15}$$

All eigenvalues are nonzero in this case, but two are degenerate. Thus, this possibility must be discarded since charged leptons are highly nondegenerate in mass, contradicting observation.

4.3.2 ℓ_L singlets, l_R triplet

This possibility contains several cases, due to the existence of three singlet irreps of A_4, to which each of the ℓ_L doublets can be assigned. It can be concluded easily that, due to the form of the invariants of (4.7), if at least two of the ℓ_L doublets are assigned the same singlet representation then the resulting mass matrix will have linearly dependent lines and thus be singular. Then, we can reduce the cases to $(e_L, \mu_L, \tau_L) \sim (\mathbf{1}, \mathbf{1}', \mathbf{1}'')$ and permutations, which all yield the same eigenvalues. Given that $\overline{\psi}$ is assigned the complementary representation of ψ, so that $\overline{\psi}\psi \sim \mathbf{1}$, this assignment corresponds to $(\overline{e_L}, \overline{\mu_L}, \overline{\tau_L}) \sim (\mathbf{1}, \mathbf{1}'', \mathbf{1}')$, given the tensor products of (4.6). Thus, we obtain the Yukawa term

$$-\, y_e \overline{e_L} \left(\Phi\, l_R\right)_{\mathbf{1}} - y_\mu \overline{\mu_L} \left(\Phi\, l_R\right)_{\mathbf{1}'} - y_\tau \overline{\tau_L} \left(\Phi\, l_R\right)_{\mathbf{1}''} + \text{H.c.}\,, \tag{4.16}$$

where the bold subscript indicates which field combination is chosen from the decomposition of the field product in parentheses. Expanding the tensor products, we obtain after SSB

$$-\begin{pmatrix} \overline{e_L} & \overline{\mu_L} & \overline{\tau_L} \end{pmatrix} \begin{pmatrix} y_e v_1 & y_e v_2 & y_e v_3 \\ y_\mu v_1 & \omega^2 y_\mu v_2 & \omega y_\mu v_3 \\ y_\tau v_1 & \omega y_\tau v_2 & \omega^2 y_\tau v_3 \end{pmatrix} \begin{pmatrix} e_R \\ \mu_R \\ \tau_R \end{pmatrix} + \text{H.c.}\,. \tag{4.17}$$

The matrix $\mathbf{M}^l \mathbf{M}^{l^\dagger}$ has characteristic polynomial

$$\lambda^3 - \lambda^2 \left(y_e^2 + y_\mu^2 + y_\tau^2\right) \left(|v_1|^2 + |v_2|^2 + |v_3|^2\right) + 3\lambda \left(y_e^2 y_\mu^2 + y_\mu^2 y_\tau^2 + y_e^2 y_\tau^2\right) \left(|v_1 v_2|^2 + |v_2 v_3|^2 + |v_1 v_3|^2\right) - 27 y_e^2 y_\mu^2 y_\tau^2 |v_1 v_2 v_3|^2 \,. \tag{4.18}$$

One of the eigenvalues is zero for the VEVs h_1 and h_4 of (4.10). For h_2 and h_3, the matrix has three distinct nonzero eigenvalues, giving the charged-lepton masses

$$m_1^e = \sqrt{3} y_e v \;\;,\;\; m_2^e = \sqrt{3} y_\mu v \;\;,\;\; m_3^e = \sqrt{3} y_\tau v \,. \tag{4.19}$$

Thus, this possibility leads to a valid charged-lepton mass matrix.

4.3.3 ℓ_L triplet, l_R singlets

This possibility also contains several cases, this time due to the freedom in assigning the singlets to l_R. As in the previous analysis, only permutations of $(e_R, \mu_R, \tau_R) \sim (\mathbf{1}, \mathbf{1}', \mathbf{1}'')$ lead to a matrix with nonzero determinant for the general VEV (v_1, v_2, v_3). From this assignment, we obtain the Yukawa term

$$\begin{aligned} &-y_e \left(\overline{\ell_L}\Phi\right)_{\mathbf{1}} e_R - y_\mu \left(\overline{\ell_L}\Phi\right)_{\mathbf{1}''} \mu_R - y_\tau \left(\overline{\ell_L}\Phi\right)_{\mathbf{1}'} \tau_R + \text{H.c.} \\ &\xrightarrow{\text{SSB}} - \begin{pmatrix} \overline{e_L} & \overline{\mu_L} & \overline{\tau_L} \end{pmatrix} \begin{pmatrix} y_e v_1 & y_\mu v_1 & y_\tau v_1 \\ y_e v_2 & \omega y_\mu v_2 & \omega^2 y_\tau v_2 \\ y_e v_3 & \omega^2 y_\mu v_3 & \omega y_\tau v_3 \end{pmatrix} \begin{pmatrix} e_R \\ \mu_R \\ \tau_R \end{pmatrix} + \text{H.c.}\,. \end{aligned} \tag{4.20}$$

The characteristic equation for $\mathbf{M}^l \mathbf{M}^{l^\dagger}$ is identical to (4.18). Thus, this possibility also leads to a valid charged-lepton mass matrix.

4.4 Neutrino masses

The previous analysis suggests two valid options for the representation assignments of ℓ_L and l_R. The neutrino Yukawa term (4.12) imposes that the product of fields $\overline{\ell_L}\tilde{\Phi}$ contain a singlet $\mathbf{1}$ term and so ℓ_L cannot be assigned to a singlet representation, as Φ is assigned to a triplet. This eliminates one of the possible assignments and we consider from this point on $\ell_L \sim \mathbf{3}$ and $(e_R, \mu_R, \tau_R) \sim (\mathbf{1}, \mathbf{1}', \mathbf{1}'')$.

In order to obtain the neutrino mass matrix given by (3.31), it is first necessary to determine the form of the Dirac neutrino mass matrix $\mathbf{m}_D$ under A_4. This can be done using the Yukawa term (4.12). Noting that $\tilde{\Phi}^\dagger \sim \Phi \sim \mathbf{3}$, we compute the field product and obtain

$$\begin{aligned} -y_\nu \overline{\nu_R} \left(\tilde{\Phi}^\dagger \ell_L\right)_{\mathbf{1}} + \text{H.c.} &= -y_\nu \overline{\nu_R} \left(\tilde{\phi_1^\dagger} e_L + \tilde{\phi_2^\dagger} \mu_L + \tilde{\phi_3^\dagger} \tau_L\right) + \text{H.c.} \\ &\xrightarrow{SSB} -y_\nu \overline{\nu_R} \left(v_1 \nu_{eL} + v_2 \nu_{\mu L} + v_3 \nu_{\tau L}\right) + \text{H.c.}\,, \end{aligned} \tag{4.21}$$

for a general VEV (v_1, v_2, v_3). Thus,

$$\mathbf{m}_D \equiv v_i \mathbf{Y}^{\nu i} = y_\nu \begin{pmatrix} v_1 \\ v_2 \\ v_3 \end{pmatrix}\,, \tag{4.22}$$

and the neutrino mass matrix is given by

$$\mathbf{m}_\nu = -v_i v_j \mathbf{Y}^{\nu i} \mathbf{Y}^{\nu j^T} M_R^{-1} = -\frac{y_\nu^2}{M_R} \begin{pmatrix} v_1^2 & v_1 v_2 & v_1 v_3 \\ v_1 v_2 & v_2^2 & v_2 v_3 \\ v_1 v_3 & v_2 v_3 & v_3^2 \end{pmatrix}\,. \tag{4.23}$$

It is clear that this matrix is singular. In fact, only one of its eigenvalues is nonzero,

$$m_1^\nu = m_2^\nu = 0\ ,\ m_3^\nu = -\frac{y_\nu^2}{M_R}\left(v_1^2 + v_2^2 + v_3^2\right)\,. \tag{4.24}$$

We conclude that the mass matrix of (4.23) does not reproduce the experimental results presented in Table 3.1, as it does not lead to three distinct nonzero mass-squared differences.

4.5 Renormalization group equations

We have concluded that, although we have increased the number of Higgs doublets to three, the implementation of the type I seesaw mechanism with one RH neutrino does not lead to a neutrino mass matrix compatible with the most recent neutrino data. However, it is important to note that the mass matrix in (4.23) is given at the seesaw scale M_R, the large energy scale at which the seesaw mechanism operates. In comparison, experimental measurements of neutrino phenomena are performed at a much lower energy scale.

The neutrino masses at the seesaw scale, given by the eigenvalues of the mass matrix of (4.23), do not coincide with the neutrino masses at the energy scale of current experiments. Rather, these masses are related through the renormalization group equations (RGE), a set of first-order differential equations which determine the evolution of the couplings of a model with energy scale. In order to determine the evolution of the neutrino masses, we must study the RGE of the flavor coupling matrices κ^{ij} introduced in Section 3.3. Recalling that

$$\mathbf{m}_\nu = -v_i v_j \kappa^{ij} \Rightarrow \kappa^{ij} = M_R^{-1} \mathbf{Y}^{\nu i} \mathbf{Y}^{\nu j^T} \,, \tag{4.25}$$

we see that neutrino masses will take different values at different energy scales according to the RGE for κ^{ij}, given by [49]

$$\begin{aligned} 16\pi^2 \frac{d\kappa^{ij}}{dt} =& -3g^2\kappa^{ij} + 4\sum_{k,l=1}^{n_H} \lambda_{kilj}\kappa^{kl} + \sum_{k=1}^{n_H} \left[T_{ki}\kappa^{kj} + T_{kj}\kappa^{ik}\right] + \kappa^{ij}P + P^T\kappa^{ij} \\ &+ 2\sum_{k=1}^{n_H} \left\{ \kappa^{kj} Y_i^{l^\dagger} Y_k^l - \left[\kappa^{ik} + \kappa^{ki}\right] Y_j^{l^\dagger} Y_k^l + Y_k^{l^T} Y_j^{l^*} \kappa^{ik} - Y_k^{l^T} Y_i^{l^*} \left[\kappa^{kj} + \kappa^{jk}\right] \right\} \,, \end{aligned} \tag{4.26}$$

where λ_{ijkl} are the couplings of the scalar potential, related to the parameters λ_i $(i = 1, 2, 3, 4)$ of (4.9), $t = \log \mu$, μ is the energy scale and

$$T_{ij} \equiv \mathrm{Tr}\left(Y_i^l Y_j^{l^\dagger}\right) \;\;,\;\; P \equiv \frac{1}{2}\sum_{k=1}^{n_H} Y_k^{l^\dagger} Y_k^l \,. \tag{4.27}$$

Y_i^l are the charged-lepton Yukawa matrices. In order to solve (4.26), it is necessary to simultaneously solve the RGE for all couplings occurring in the equation. Thus, we also need the RGE for λ_{ijkl}, Y_i^l, and g, as well as additional couplings which may arise in these equations. For a simpler analysis, we consider a leading-log approximation to the RGE of (4.26), with the assumption that the terms on the right-hand side of the equation are constant. Under this approximation, κ^{ij} evolves according to

$$\kappa^{ij}(\mu) = \kappa^{ij}(M_R) + \left.\frac{d\kappa^{ij}}{dt}\right|_{t=\log M_R} \log(\mu/M_R) \,, \tag{4.28}$$

where

$$\kappa^{ij}(M_R) = \frac{y_\nu^2}{M_R}\begin{pmatrix} \delta_{i1}\delta_{j1} & \delta_{i1}\delta_{j2} & \delta_{i1}\delta_{j3} \\ \delta_{i2}\delta_{j1} & \delta_{i2}\delta_{j2} & \delta_{i2}\delta_{j3} \\ \delta_{i3}\delta_{j1} & \delta_{i3}\delta_{j2} & \delta_{i3}\delta_{j3} \end{pmatrix}, \tag{4.29}$$

and δ_{ij} is the Kronecker delta. The mass matrix at the energy scale of current experiments (which we take to be m_Z) is simply

$$\mathbf{m}_\nu(m_Z) = -v_i v_j \kappa^{ij}(m_Z)\,, \tag{4.30}$$

from which we conclude that all effective operators κ^{ij} contribute, in principle, to neutrino masses and mixing.

4.5.1 Truncated RGE

Let us begin by considering a truncated form of (4.26), taking only the first two terms on the right-hand side. These should be the most important, as all remaning terms contain the charged-lepton Yukawa matrices, of smaller order of magnitude. This means that we are interested in those cases with $y_l \sim \frac{m_l}{v} \ll g, \lambda_{ijkl} \sim 1$.

The calculation of the mass matrix must be performed for each of the two VEVs that lead to a valid charged-lepton mass matrix, i.e., $h_2 = v(1,1,1)$ and $h_3 = v(\pm 1, \eta, \eta^*)$. For h_2, we obtain the mass matrix

$$\mathbf{m}_\nu = -\frac{v^2 y_\nu^2}{M_R}\begin{pmatrix} x & y & y \\ y & x & y \\ y & y & x \end{pmatrix}, \tag{4.31}$$

where

$$x = 1 + \left\{-3g^2 + 4\left[\lambda_{aaaa} + 2\,\mathrm{Re}\left(\lambda_{abab}\right)\right]\right\}\frac{\log(m_Z/M_R)}{16\pi^2}\,, \tag{4.32}$$

$$y = 1 + \left[-3g^2 + 4\left(\lambda_{aabb} + \lambda_{abba}\right)\right]\frac{\log(m_Z/M_R)}{16\pi^2}\,, \tag{4.33}$$

being the λ parameters given in Table 4.2. The eigenvalues of (4.31) are

$$m_1^\nu = m_2^\nu = -\frac{v^2 y_\nu^2}{M_R}(x-y)\ ,\ m_3^\nu = -\frac{v^2 y_\nu^2}{M_R}(x+2y)\,. \tag{4.34}$$

There are two degenerate eigenvalues, thus we do not obtain three nondegenerate nonzero mass-squared differences. For the remaining VEV configuration, h_3, we obtain the mass matrix

$$\mathbf{m}_\nu = -\frac{v^2 y_\nu^2}{M_R}\begin{pmatrix} x' & \pm\eta y & \pm\eta^* y \\ \pm\eta y & \omega x' & y \\ \pm\eta^* y & y & \omega^* x' \end{pmatrix}, \tag{4.35}$$

with

$$x' = 1 + \left\{-3g^2 + 4\left[\lambda_{aaaa} + 2\,\mathrm{Re}\left(\omega\lambda_{abab}\right)\right]\right\}\frac{\log(m_Z/M_R)}{16\pi^2}\,. \tag{4.36}$$

Given that this matrix is complex, we must determine the eigenvalues of $\mathbf{m}_\nu \mathbf{m}_\nu^\dagger$, which takes the form

$$\mathbf{m}_\nu \mathbf{m}_\nu^\dagger = \frac{v^4 y_\nu^4}{M_R^2} \begin{pmatrix} x'^2 + 2y^2 & \pm\eta^* \left(2x'y + y^2\right) & \pm\eta \left(2x'y + y^2\right) \\ \pm\eta \left(2x'y + y^2\right) & x'^2 + 2y^2 & \omega \left(2x'y + y^2\right) \\ \pm\eta^* \left(2x'y + y^2\right) & \omega^* \left(2x'y + y^2\right) & x'^2 + 2y^2 \end{pmatrix} . \tag{4.37}$$

The eigenvalues are

$$m_1^\nu = m_2^\nu = \frac{v^2 y_\nu^2}{M_R} \left|x' - y\right| \ , \ m_3^\nu = \frac{v^2 y_\nu^2}{M_R} \left|x' + 2y\right| . \tag{4.38}$$

There are two degenerate eigenvalues in this case as well. Having exhausted the possibilities, we conclude that it is not possible to obtain three distinct nonzero neutrino mass-squared differences by applying a leading-log approximation to the truncated form of the RGE (4.26). We verify that, in this case, the degenerate eigenvalues of the mass matrix are no longer zero. We move on to an application of the entire RGE, in the hope that this final step will lift the degeneracy and result in three distinct neutrino masses.

4.5.2 Full RGE

The full RGE includes the remaining terms of (4.26), containing the charged-lepton Yukawa matrices. These matrices should lead to smaller corrective terms to the larger terms previously considered. As a result, it is a reasonable approximation to consider $y_e, y_\mu \to 0$ and obtain the correction as a function of y_τ, the larger of the charged-lepton Yukawa constants. Under this condition, we obtain the Yukawa matrices

$$Y_1^l \approx \begin{pmatrix} 0 & 0 & y_\tau \\ 0 & 0 & 0 \\ 0 & 0 & 0 \end{pmatrix} \ , \ Y_2^l \approx \begin{pmatrix} 0 & 0 & 0 \\ 0 & 0 & \omega^2 y_\tau \\ 0 & 0 & 0 \end{pmatrix} \ , \ Y_3^l \approx \begin{pmatrix} 0 & 0 & 0 \\ 0 & 0 & 0 \\ 0 & 0 & \omega y_\tau \end{pmatrix} . \tag{4.39}$$

Using (4.27), we determine

$$P = \frac{3}{2} \begin{pmatrix} 0 & 0 & 0 \\ 0 & 0 & 0 \\ 0 & 0 & y_\tau^2 \end{pmatrix} \ , \ T_{ij} = y_\tau^2 \delta_{ij} . \tag{4.40}$$

We use the results above to obtain the matrices A^{ij} such that (4.26) can be rewritten as

$$16\pi^2 \frac{d\kappa^{ij}}{dt} = -3g^2 \kappa^{ij} + 4 \sum_{k,l=1}^{n_H} \lambda_{kilj} \kappa^{kl} + \frac{y_\nu^2}{M_R} A^{ij} . \tag{4.41}$$

In this way, we can add the corrective term

$$- v_i v_j \frac{y_\nu^2}{16\pi^2 M_R} A^{ij} \log(m_Z / M_R) , \tag{4.42}$$

to (4.31) and (4.35) to obtain the neutrino mass matrices. In the above equations, the matrices A^{ij} are given by

$$A^{ij} = y_\tau^2 \begin{pmatrix} 2\delta_{i1}\delta_{j1} & 2\delta_{i1}\delta_{j2} & \frac{7}{2}\delta_{i1}\delta_{j3} - 2\delta_{i3}\delta_{j1} \\ 2\delta_{i2}\delta_{j1} & 2\delta_{i2}\delta_{j2} & \frac{7}{2}\delta_{i2}\delta_{j3} - 2\delta_{i3}\delta_{j2} \\ \frac{7}{2}\delta_{i3}\delta_{j1} - 2\delta_{i1}\delta_{j3} & \frac{7}{2}\delta_{i3}\delta_{j2} - 2\delta_{i2}\delta_{j3} & \delta_{i3}\delta_{j3} \end{pmatrix} . \tag{4.43}$$

In the end, for the VEV h_2, we obtain

$$\mathbf{m}_\nu = -\frac{v^2 y_\nu^2}{M_R} \begin{pmatrix} x + 2\delta_c & y + 2\delta_c & y + \frac{3}{2}\delta_c \\ y + 2\delta_c & x + 2\delta_c & y + \frac{3}{2}\delta_c \\ y + \frac{3}{2}\delta_c & y + \frac{3}{2}\delta_c & x + \delta_c \end{pmatrix} \ , \ \delta_c = \frac{y_\tau^2}{16\pi^2}\log(m_Z/M_R)\,, \tag{4.44}$$

with eigenvalues

$$\begin{aligned} m_1^\nu &\simeq -\frac{v^2 y_\nu^2}{M_R}\,(x - y)\ , \\ m_2^\nu &\simeq -\frac{v^2 y_\nu^2}{2M_R}\left(y + 2x + 5\delta_c - \sqrt{3}\sqrt{3y^2 + 10y\delta_c + 9\delta_c^2}\right)\ , \\ m_3^\nu &\simeq -\frac{v^2 y_\nu^2}{2M_R}\left(y + 2x + 5\delta_c + \sqrt{3}\sqrt{3y^2 + 10y\delta_c + 9\delta_c^2}\right)\ . \end{aligned} \tag{4.45}$$

We conclude that the inclusion of the correctional term δ_c, arising from the Yukawa terms in the RGE of κ^{ij}, lifts the degeneracy among the eigenvalues. In this case, we obtain three distinct eigenvalues which can be used to compute the neutrino mass-squared differences. Before moving on, we determine the corrected mass matrix for the VEV h_3, which reads

$$\mathbf{m}_\nu = -\frac{v^2 y_\nu^2}{M_R} \begin{pmatrix} x' + 2\delta_c & \pm\eta(y + 2\delta_c) & \pm\eta^*(y + 3/2\delta_c) \\ \pm\eta(y + 2\delta_c) & \omega(x' + 2\delta_c) & y + 3/2\delta_c \\ \pm\eta^*(y + 3/2\delta_c) & y + 3/2\delta_c & \omega^*(x' + \delta_c) \end{pmatrix} . \tag{4.46}$$

Computing $\mathbf{m}_\nu \mathbf{m}_\nu^\dagger$ and determining its eigenvalues, we find

$$\begin{aligned} m_1^\nu &\simeq \frac{v^2 y_\nu^2}{M_R}\,|x' - y|\ , \\ m_2^\nu &\simeq \frac{v^2 y_\nu^2}{2M_R}\left|y + 2x' + 5\delta_c - \sqrt{3}\sqrt{3y^2 + 10y\delta_c + 9\delta_c^2}\right|\ , \\ m_3^\nu &\simeq \frac{v^2 y_\nu^2}{2M_R}\left|y + 2x' + 5\delta_c + \sqrt{3}\sqrt{3y^2 + 10y\delta_c + 9\delta_c^2}\right|\ . \end{aligned} \tag{4.47}$$

We have thus determined the neutrino mass matrices at the energy scale of current experiments for each of the two valid Higgs VEV configurations, concluding in both cases that they have three nondegenerate eigenvalues, corresponding to three distinct neutrino masses. We now move on to test these results by comparing them with the experimental data available, as presented in Table 3.1. This must be done with some care, as the values x, x', y and δ_c can take are not entirely free. In fact, δ_c is constant once the seesaw scale $\Lambda = M_R$ is fixed. The remaining three parameters are functions of the couplings λ_{ijkl}, which are related to the parameters of the scalar potential, and are restricted to the region of the parameter space where each VEV is valid. In order to take these restrictions into account, we study the

problem numerically, by generating points in the parameter space, in the regions of validity of each VEV. For those points we determine the corresponding neutrino masses.

4.6 Numerical analysis

In order to test the results of the model, we must compare the neutrino masses obtained after application of the RGE with the experimental data available. Since there are no experimental values for neutrino masses, we use mass-squared differences. Actually, we take into account the ratio

$$R = \frac{\Delta m^2_{21}}{|\Delta m^2_{3\ell}|}\,, \tag{4.48}$$

using the values in Table 3.1. By comparing this ratio, we test the parameters of the model contained in x, x', y without concerning ourselves with the normalization provided by y_ν, M_R.

In order to perform this test, we wrote a C++ program which, for each of the valid VEVs h_2 and h_3, generates with each iteration a point randomly in the region of the parameter space where the VEV is valid. It then uses the couplings λ_{ijkl} associated with that point to determine the right-hand side of (4.26), considering the full Yukawa terms and the seesaw scale $M_R = 10^{14}$ GeV. The program calculates $\mathbf{m}_\nu$ and $\mathbf{m}_\nu\mathbf{m}_\nu^\dagger$, then obtains the eigenvalues of the Hermitian mass matrix, corresponding to the squared neutrino masses. Finally, it identifies the type of ordering, which can be normal or inverted, as defined in (3.11), and obtains the ratio R.

The regions of validity of the VEVs are presented in [54], which uses a scalar potential with a different parametrization from the one used in this thesis, related to the parametrization of (4.9) through

$$m^2 = -\frac{M_0}{\sqrt{3}}\ ,\ \lambda_1 = \frac{2}{3}\Lambda_0\ ,\ \lambda_2 = \frac{\Lambda_3}{3}\ ,\ \lambda_3 = \frac{\Lambda_1+\Lambda_2}{2}\ ,\ \lambda_4' = \frac{\Lambda_1-\Lambda_2}{2} - i\frac{\Lambda_4}{2}\,. \tag{4.49}$$

The regions of validity for the two VEVs are [54]

$$h_2 = v(1,1,1) \to \begin{cases} \Lambda_4^2 < 12\Lambda_1^2 \\ \Lambda_4^2 < 2(\Lambda_3 + |\Lambda_1|)(\Lambda_2 + |\Lambda_1|) \\ \Lambda_1 < 0 \\ \Lambda_0 > |\Lambda_1| > -\Lambda_2, -\Lambda_3 \end{cases} \quad,\quad h_3 = v(\pm 1, \eta, \eta^*) \to \begin{cases} \Lambda_2 < 0 \\ |\Lambda_2| > |\Lambda_1| \\ \Lambda_3 > \Lambda_1 \\ 4\Lambda_0 + \Lambda_1 > 3|\Lambda_2| \end{cases}\,. \tag{4.50}$$

Rather than convert these conditions to the parameters λ_i, we use the parameters Λ_i in the program. Having established the conversion between parametrizations, we can determine the couplings λ_{ijkl} from the parameters Λ_i, as indicated in Table 4.2.

Upon running the program, we verify that the ratio R is never obtained for either of the VEVs h_2 and h_3, despite the large number of iterations considered. In fact, the ratio is found to be $R \sim 10^{-12}$, much lower than the experimental value (≈ 0.03) and, given the limited precision of the program used, compatible with $R = 0$. This result is not surprising, as it has been shown [55] that it is not possible to obtain

λ_{ijkl}	$f(\lambda_i)$	$f(\Lambda_i)$
λ_{aaaa} $(i=j=k=l)$	$\lambda_1/2+\lambda_2$	$\Lambda_0/3+\Lambda_3/3$
λ_{aabb} $(i=j\neq k=l)$	$\lambda_1/2-\lambda_2/2$	$\Lambda_0/3-\Lambda_3/6$
λ_{abba} $(i=l\neq j=k)$	$\lambda_3/2$	$\Lambda_1/4+\Lambda_2/4$
λ_{abab} $(i=k\neq j=l)$	$\lambda_4'/2$	$\Lambda_1/4-\Lambda_2/4-i\Lambda_4/2$
$\overline{\lambda}_{abab}$ $(i=k\neq j=l)$	$\lambda_4'^*/2$	$\Lambda_1/4-\Lambda_2/4+i\Lambda_4/2$
otherwise		0

Table 4.2: Correspondence between the couplings λ_{ijkl}, the parameters λ_i of the scalar potential of (4.9) and the parameters Λ_i of the scalar potential of [54]. λ_{abab} corresponds to the cases where $b = a+1(\text{mod }3)$ and $\overline{\lambda}_{abab}$ to the cases where $b=a-1(\text{mod }3)$.

three nondegenerate neutrino masses in a model with A_4 symmetry, three scalar doublets in a triplet, and three lepton families. This might come into apparent conflict with the seemingly nondegenerate eigenvalues of (4.45), but if we perform an expansion in powers of δ_c, we obtain

$$-\frac{2M_R}{v^2y_\nu^2}m_{2,3}^\nu = 2x+(y\pm 3y)+(5\delta_c\pm 5\delta_c)+\mathcal{O}\left(\delta_c^2\right)\ . \tag{4.51}$$

Thus, the degeneracy between the approximate eigenvalues m_1^ν and m_2^ν can only be lifted by terms in $\mathcal{O}\left(\delta_c^2\right)$, where $x, x', y \sim 1$ and $\delta_c \sim 10^{-5}$. It is quite possible that this small correction is only present in the approximate eigenvalues, having arisen from the approximations themselves, and that the exact solution of the RGE remains degenerate, in agreement with the conclusions of [55]. Thus, we conclude that the effect of the corrections originated from the charged-lepton Yukawa matrices does not cause a splitting of eigenvalues capable of reproducing experimental data.

The results above lead to the conclusion that the model as was formulated is incapable of reproducing the available experimental results and, by extension, is not valid. The model's apparent resistance to a split in the two degenerate neutrino masses would suggest that this degeneracy is protected by the A_4 symmetry, which is only broken at low energies. The running of the couplings is performed on a model which is invariant under A_4, causing the effect of the RGE on the degeneracy of the neutrino masses to be negligible. It is then clear that, if we were able to break the A_4 symmetry in some way above the seesaw scale, we would obtain a much greater range of values available to R, as the degeneracy between neutrino masses would no longer be protected during the running of the couplings. This can be achieved by adding a term which is not invariant under A_4 to the model Lagrangian, causing the A_4 symmetry to be (softly) broken. The soft breaking of the A_4 symmetry of the model is the topic of the next chapter, which focuses on mechanisms that give rise to soft breaking terms, and their effects on the neutrino parameters at low energies.

Chapter 5

Softly-broken single right-handed neutrino A_4 model

Given that the model presented in the previous chapter failed to reproduce neutrino data, we now introduce a slight alteration. We consider the effect of adding a new Lagrangian term which breaks the A_4 symmetry softly. This can in principle be done either in the fermion or scalar sectors. By breaking the A_4 symmetry above the seesaw scale M_R, the degeneracy between neutrino masses will no longer be protected as RGEs are applied, causing the neutrino mass-squared differences at the low energy scale m_Z to take on a larger range of values. This should lead to valid results for the ratio R, upon which we move on to study the remaining parameters of the low-energy neutrino sector, namely the mixing angles θ_{ij} of the PMNS matrix defined in (3.10).

In the present model, a fermionic A_4-symmetry breaking term can be introduced in the heavy neutrino masses

$$-\frac{1}{2}M_R\overline{\nu_R}\nu_R^C + \text{H.c.}\,, \tag{5.1}$$

or in the Yukawa term (4.12). The field product of (5.1) is of the form $\mathbf{1}\otimes\mathbf{1}=\mathbf{1}$, thus there is no way to obtain from (5.1) a term that is not invariant under A_4. The field product of (4.12), on the other hand, is of the form $\mathbf{3}\otimes\mathbf{3}\otimes\mathbf{1}=\mathbf{1}\oplus\mathbf{1}'\oplus\mathbf{1}''\oplus\mathbf{3}\oplus\mathbf{3}$. Thus, it is possible to define a Yukawa term that breaks A_4, by selecting the singlet components $\mathbf{1}'$ or $\mathbf{1}''$. However, given that the Yukawa term is of dimension 4, a term of this form leads to hard symmetry breaking rather than soft breaking and is, therefore, not an option. This leaves us with the possibility of soft breaking in the scalar sector, which will occupy the remainder of the chapter.

5.1 A simple soft breaking scheme in the scalar sector

We consider the addition of an A_4-breaking term in the scalar potential. The alteration of $V(\Phi)$ changes the conditions of minimization of the potential, so that the VEV configurations which lead to a global minimum should be altered in relation to (4.10). The structure of the valid VEVs h_2 and h_3 satisfies

$|v_1| = |v_2| = |v_3|$. Thus, even a small correction which results in the breaking of this pattern could lead to richer results in the neutrino mass spectrum at low energies.

Following the procedure described in [56], we introduce three scalar singlet fields assigned to a triplet of A_4, $\Psi \sim \mathbf{3}$. Under the assumption that

$$\langle \Psi \rangle \gg v \,, \tag{5.2}$$

we can establish that the potential for Ψ decouples from $V(\Phi)$. Thus, $V(\Psi)$ has the structure of (4.9) and its VEVs are those of (4.10). Let us consider $\langle \Psi \rangle \sim (1,0,0)$. When Ψ acquires a VEV, only the singlet components of the field product $(\Psi^\dagger \Psi)$ are nonzero, as can be concluded from the invariants in (4.7). After SSB in $V(\Psi)$, the surviving interaction terms between the scalar fields Φ and Ψ are

$$\begin{aligned} \lambda_a (\Psi^\dagger \Psi)_{\mathbf{1}''} (\Phi^\dagger \Phi)_{\mathbf{1}'} + \text{H.c.} &\xrightarrow{\text{SSB}} M_S^2 \left[(\Phi^\dagger \Phi)_{\mathbf{1}'} + \text{H.c.} \right] \,, \\ \lambda_b (\Psi^\dagger \Psi)_{\mathbf{1}} (\Phi^\dagger \Phi)_{\mathbf{1}} &\xrightarrow{\text{SSB}} M_\mu^2 (\Phi^\dagger \Phi)_{\mathbf{1}} \,. \end{aligned} \tag{5.3}$$

The second interaction term simply redefines m^2 in (4.9), while the first term becomes an A_4-breaking term in the scalar potential $V(\Phi)$. Thus, the soft-breaking potential $V_{\text{SB}}(\Phi)$ obtained by adding Ψ is

$$V_{\text{SB}}(\Phi) = V(\Phi) + M_S^2 \left(2\phi_1^\dagger \phi_1 - \phi_2^\dagger \phi_2 - \phi_3^\dagger \phi_3 \right) \,. \tag{5.4}$$

Under this potential, the Higgs obtains a VEV configuration of the form

$$\langle \Phi \rangle \equiv h_5 = v(1 + 2\varepsilon, 1 - \varepsilon, 1 - \varepsilon) \,, \tag{5.5}$$

where $\varepsilon \sim M_S^2 / v^2$. The new parameter ε provides a correction to the form of the VEV $h_2 = v(1,1,1)$ such that we obtain $|v_1| \neq |v_2|, |v_3|$. Therefore, we must study the model considering this new VEV. The first step is to obtain the new charged-lepton mass matrix and its eigenvalues, necessary to determine the form of the charged-lepton Yukawa matrices $\mathbf{Y}^l$ and the Yukawa constants y_l.

5.1.1 Charged-lepton masses

We recall the charged-lepton mass matrix $\mathbf{M}^l$ obtained in Section 4.3.3, to which corresponds the Hermitian matrix

$$\mathbf{H}^l = \mathbf{M}^l \mathbf{M}^{l\dagger} = \begin{pmatrix} |v_1|^2 (y_e^2 + y_\mu^2 + y_\tau^2) & v_1 v_2^* (y_e^2 + \omega^2 y_\mu^2 + \omega y_\tau^2) & v_1 v_3^* (y_e^2 + \omega y_\mu^2 + \omega^2 y_\tau^2) \\ v_1^* v_2 (y_e^2 + \omega y_\mu^2 + \omega^2 y_\tau^2) & |v_2|^2 (y_e^2 + y_\mu^2 + y_\tau^2) & v_2 v_3^* (y_e^2 + \omega^2 y_\mu^2 + \omega y_\tau^2) \\ v_1^* v_3 (y_e^2 + \omega^2 y_\mu^2 + \omega y_\tau^2) & v_2^* v_3 (y_e^2 + \omega y_\mu^2 + \omega^2 y_\tau^2) & |v_3|^2 (y_e^2 + y_\mu^2 + y_\tau^2) \end{pmatrix} \,. \tag{5.6}$$

For the VEVs of the A_4-symmetric potential, the eigenvalues of $\mathbf{H}^l$ can be determined analytically. For the new VEV h_5, this is no longer the case. We resort to determining the eigenvalues using perturbation theory, under the assumption that the Yukawa constants y_e, y_μ, y_τ are small enough for the results to converge. We consider as the unperturbed matrix $\mathbf{H}_0$ the one obtained from $\mathbf{H}^l$ by setting $y_e \to 0$. The

perturbation will consequently be given by $\mathbf{H}_{\mathsf{P}} = \mathbf{H}^l - \mathbf{H}_0$, such that

$$\mathbf{H}_0 = \begin{pmatrix} |v_1|^2(y_\mu^2+y_\tau^2) & v_1v_2^*(\omega^2y_\mu^2+\omega y_\tau^2) & v_1v_3^*(\omega y_\mu^2+\omega^2y_\tau^2) \\ v_1^*v_2(\omega y_\mu^2+\omega^2y_\tau^2) & |v_2|^2(y_\mu^2+y_\tau^2) & v_2v_3^*(\omega^2y_\mu^2+\omega y_\tau^2) \\ v_1^*v_3(\omega^2y_\mu^2+\omega y_\tau^2) & v_2^*v_3(\omega y_\mu^2+\omega^2y_\tau^2) & |v_3|^2(y_\mu^2+y_\tau^2) \end{pmatrix}, \; \mathbf{H}_{\mathsf{P}} = y_e^2 \begin{pmatrix} |v_1|^2 & v_1v_2^* & v_1v_3^* \\ v_1^*v_2 & |v_2|^2 & v_2v_3^* \\ v_1^*v_3 & v_2^*v_3 & |v_3|^2 \end{pmatrix}. \tag{5.7}$$

We determine the eigenvalues and eigenvectors of $\mathbf{H}_0$ analytically and, using first-order perturbation theory, we obtain the eigenvalues of $\mathbf{H}^l$, from which we extract the ones of $\mathbf{M}^l$. Namely,

$$\begin{aligned} (m_1^e)^2 &\simeq 3v^2y_e^2\frac{(1+\varepsilon-2\varepsilon^2)^2}{1+\varepsilon(2+3\varepsilon)}\,, \\ (m_2^e)^2 &\simeq 3v^2y_\mu^2\frac{1+\varepsilon^3(3\varepsilon-4)}{1+2\varepsilon^2}+\mathcal{O}(y_e^2)+\mathcal{O}(y_\mu^4)\,, \\ (m_3^e)^2 &\simeq 3v^2y_\mu^2\frac{\varepsilon^2(2+\varepsilon)^2}{1+2\varepsilon^2}+3v^2y_\tau^2(1+2\varepsilon^2)+\mathcal{O}(y_e^2)+\mathcal{O}(y_\mu^4)\,, \end{aligned} \tag{5.8}$$

where the identification $m_{1,2,3}^e \equiv m_{e,\mu,\tau}$ can be used to compute the Yukawa constants y_e, y_μ and y_τ, which in turn allow us to determine the charged-lepton Yukawa matrices, present in the κ^{ij} RGE. We obtain

$$\begin{aligned} y_e^2 &\simeq \frac{m_e^2}{3v^2}\frac{1+\varepsilon(2+3\varepsilon)}{(1+\varepsilon-2\varepsilon^2)^2}\,, \\ y_\mu^2 &\simeq \frac{m_\mu^2}{3v^2}\frac{1+2\varepsilon^2}{1+\varepsilon^3(3\varepsilon-4)}\,, \\ y_\tau^2 &\simeq -\frac{m_\mu^2}{3v^2}\frac{\varepsilon^2(2+\varepsilon)^2}{(1+2\varepsilon^2)(\varepsilon-1)^2[1+\varepsilon(2+3\varepsilon)]}+\frac{m_\tau^2}{3v^2}\frac{1}{1+2\varepsilon^2}\,, \end{aligned} \tag{5.9}$$

showing that the Yukawa couplings maintain the relation $y_l^2 \sim \frac{m_l^2}{3v^2}$ found in (4.19) for the VEVs h_2 and h_3 of (4.10), corrected by a function of ε in the case of the VEV h_5. Thus, our initial assumption that y_l are small enough to allow the application of perturbation theory is validated.

5.1.2 Lepton mixing

In order to study the results for the new VEV h_5 (obtained by adding a soft-breaking term in the effective Higgs scalar potential), we can use the computer code described in Section 4.6, with some changes. In addition to changing the VEV, we must also use the results of Section 5.1.1 to define the new charged-lepton Yukawa matrices. The parameter ε is generated randomly, such that $|\varepsilon| < 3$. We run the program and obtain the results presented in Figure 5.1, for the NO case. For inverted ordering, R is always outside the allowed range.

We conclude that the soft breaking of A_4 in the scalar sector introduced a large enough split between the degenerate neutrino masses, so that we obtain values of R within the 3σ and 1σ allowed intervals given in Table 3.1. This happens for a wide range of values for ε. There is a lack of points around $\varepsilon = 0$, where the VEV configuration h_5 coincides with h_2, and around $\varepsilon = 1$, where $h_5 = h_1$, so the result is expected in both cases. There is a large region around $\varepsilon = -2$ where there are no valid results for R,

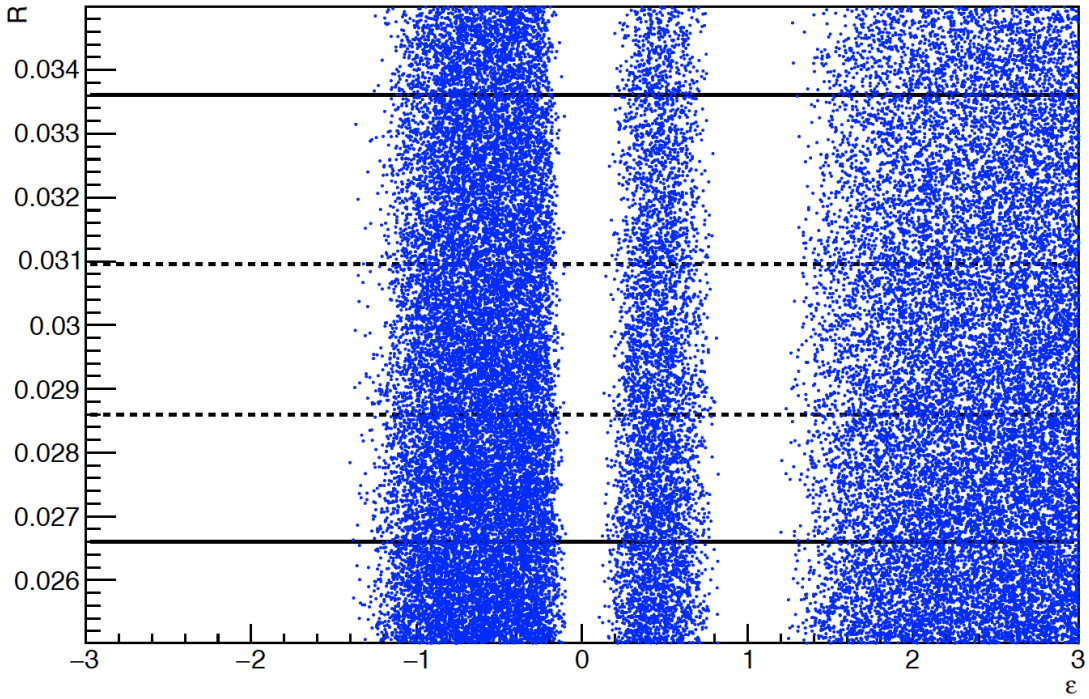

Figure 5.1: Values obtained for R, ε after RGE running of κ^{ij} and using h_5 for $\langle\Phi\rangle$, for the NO case. The solid (dashed) horizontal lines enclose the 3σ (1σ) allowed interval for R.

since $h_5 \to (-1,1,1)$, a configuration for which $|v_1| = |v_2| = |v_3|$.

Having obtained valid results for R, we continue the analysis of the model by studying the PMNS matrix. As described in Section 3.1, the PMNS matrix U is obtained from the unitary transformations that diagonalize the lepton mass matrices, through (3.9). Once U is obtained, the mixing angles can be recovered following the procedure outlined in Appendix A of [57]. The mixing matrix obtained by our code is of the form

$$\begin{gathered} U = \text{diag}(e^{i\delta_e}, e^{i\delta_\mu}, e^{i\delta_\tau}) \cdot V \cdot \text{diag}(e^{-i\alpha_1/2}, e^{-i\alpha_2/2}, 1)\,, \\ V = \begin{pmatrix} c_{12}c_{13} & s_{12}c_{13} & s_{13}e^{-i\delta} \\ -s_{12}c_{23} - c_{12}s_{23}s_{13}e^{i\delta} & c_{12}c_{23} - s_{12}s_{23}s_{13}e^{i\delta} & s_{23}c_{13} \\ s_{12}s_{23} - c_{12}c_{23}s_{13}e^{i\delta} & -c_{12}s_{23} - s_{12}c_{23}s_{13}e^{i\delta} & c_{23}c_{13} \end{pmatrix}, \end{gathered} \tag{5.10}$$

where δ_e, δ_μ, δ_τ are unphysical phases which can be removed by rephasing the charged-lepton fields and α_1, α_2 are Majorana-type phases. The parameters of the matrix U are given by

$$\begin{gathered} \theta_{12} = \begin{cases} \arctan\left(\frac{|U_{12}|}{|U_{11}|}\right) & \text{if } U_{11} \neq 0 \\ \frac{\pi}{2} & \text{else} \end{cases}\,, \quad \theta_{23} = \begin{cases} \arctan\left(\frac{|U_{23}|}{|U_{33}|}\right) & \text{if } U_{33} \neq 0 \\ \frac{\pi}{2} & \text{else} \end{cases}\,, \quad \theta_{13} = \arcsin\left(|U_{13}|\right)\,, \\ \delta = -\text{arg}\left(\frac{\frac{U_{ii}^* U_{ij} U_{ji} U_{jj}^*}{c_{12}c_{13}^2 c_{23} s_{13}} + c_{12}c_{23}s_{13}}{s_{12}s_{23}}\right)\,, \quad \text{where } i,j \in \{1,2,3\} \text{ and } i \neq j\,, \\ \delta_e = \text{arg}\left(e^{i\delta} U_{13}\right)\,, \quad \delta_\mu = \text{arg}\left(U_{23}\right)\,, \quad \delta_\tau = \text{arg}\left(U_{33}\right)\,, \\ \alpha_1 = 2\,\text{arg}\left(e^{i\delta_e} U_{11}^*\right)\,, \quad \alpha_2 = 2\,\text{arg}\left(e^{i\delta_e} U_{12}^*\right)\,. \end{gathered} \tag{5.11}$$

From these relations, we can extract the mixing angles $\theta_{12},\ \theta_{13},\ \theta_{23}$, as well as the complex phases δ and $\alpha_1,\ \alpha_2$. We run the program and obtain the values of s^2_{ij} for all cases where the ratio R is within the 3σ allowed range. The results are presented in Figure 5.2. One can see that, although ε has a wide range of values which lead to a valid R, the results for the mixing angles are restricted to specific regions of the parameter space, which do not intersect those singled out by the experimental results. The conclusion is that no cases are found where both R and all three mixing angles are within the 3σ allowed range. Thus, we must discard h_5 as a valid VEV.

5.2 Alternative VEVs of the softly-broken A_4 potential

In the previous section, we have concluded that the VEV configuration h_5 does not lead to satisfactory results. However, this is not the end of the analysis related with soft breaking of the A_4 symmetry in the scalar sector, as the Higgs scalar potential $V_{\text{SB}}(\Phi)$ of (5.4) must have other minima, which could lead to different results for the mixing angles θ_{ij}. Thus, the next step is to minimize $V_{\text{SB}}(\Phi)$ in order to determine all VEV configurations of this potential, so that we can obtain for each of them the parameters of the low-energy neutrino sector. But first, we will investigate whether the general VEV patterns

$$h_6 = v(1, \varepsilon_1, \varepsilon_2)\,, \tag{5.12}$$

and

$$h_7 = v(1, \varepsilon_1 e^{i\theta_1}, \varepsilon_2 e^{i\theta_2})\,, \tag{5.13}$$

lead to viable results . This general analysis should give us an idea about whether it is worth it to find VEV configurations of the forms of h_6 and h_7. Once again, we must study the charged-lepton mass matrix. Applying perturbation theory as was done in Section 5.1.1, and considering the VEVs h_6 and h_7 rather than h_5, we find that the complex phases θ_1, θ_2 cancel out of the eigenvalues and the results are identical for both VEVs,

$$\begin{aligned}
(m^e_1)^2 &\simeq 9v^2 y_e^2 \frac{\varepsilon_1^2\varepsilon_2^2}{\varepsilon_1^2+\varepsilon_2^2+\varepsilon_1^2\varepsilon_2^2}\,,\\
(m^e_2)^2 &\simeq 3v^2 y_\mu^2 \frac{\varepsilon_1^2+\varepsilon_2^2+\varepsilon_1^2\varepsilon_2^2}{1+\varepsilon_1^2+\varepsilon_2^2} + \mathcal{O}(y_e^2) + \mathcal{O}(y_\mu^4)\,,\\
(m^e_3)^2 &\simeq v^2 y_\tau^2(1+\varepsilon_1^2+\varepsilon_2^2) + v^2 y_\mu^2 \frac{1-\varepsilon_1^2-\varepsilon_2^2-\varepsilon_1^2\varepsilon_2^2+\varepsilon_1^4+\varepsilon_2^4}{1+\varepsilon_1^2+\varepsilon_2^2} + \mathcal{O}(y_e^2) + \mathcal{O}(y_\mu^4)\,,
\end{aligned} \tag{5.14}$$

so that

$$\begin{aligned}
y_e^2 &\simeq \frac{m_e^2}{3v^2}\frac{\varepsilon_1^2+\varepsilon_2^2+\varepsilon_1^2\varepsilon_2^2}{3\varepsilon_1^2\varepsilon_2^2}\,,\\
y_\mu^2 &\simeq \frac{m_\mu^2}{3v^2}\frac{1+\varepsilon_1^2+\varepsilon_2^2}{\varepsilon_1^2+\varepsilon_2^2+\varepsilon_1^2\varepsilon_2^2}\,,\\
y_\tau^2 &\simeq -\frac{m_\mu^2}{3v^2}\frac{1-\varepsilon_1^2-\varepsilon_2^2-\varepsilon_1^2\varepsilon_2^2+\varepsilon_1^4+\varepsilon_2^4}{(1+\varepsilon_1^2+\varepsilon_2^2)(\varepsilon_1^2+\varepsilon_2^2+\varepsilon_1^2\varepsilon_2^2)} + \frac{m_\tau^2}{3v^2}\frac{3}{1+\varepsilon_1^2+\varepsilon_2^2}\,.
\end{aligned} \tag{5.15}$$

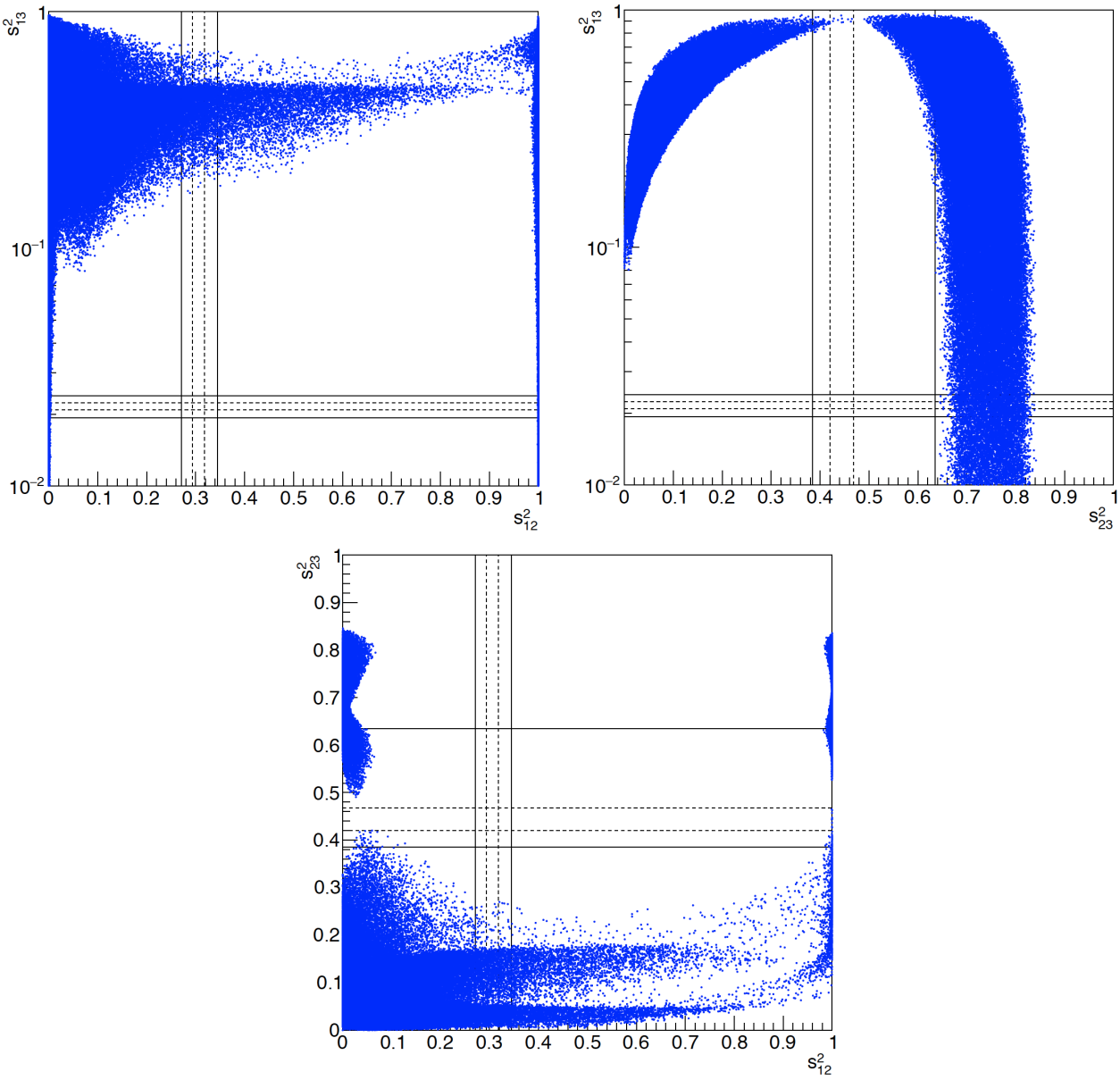

Figure 5.2: Values obtained for s^2_{ij} after RGE running of κ^{ij} and using h_5 for $\langle\Phi\rangle$. The axis corresponding to s^2_{13} is in logarithmic scale. The solid (dashed) black lines enclose the 3σ (1σ) allowed interval for each variable. In all cases R is within the 3σ experimental range.

Replacing these results in the program, we run it again. When scanning $(\varepsilon_1,\ \varepsilon_2,\ \theta_1,\ \theta_2)$, we consider $|\varepsilon_{1,2}| < 3$ and $\theta_{1,2} \in [-\pi, \pi]$. The values obtained for s^2_{ij} under the condition that R is within the 3σ allowed range are presented in Figures 5.3 and 5.4 for h_6 and h_7, respectively.

From Figure 5.3 we conclude that the regions are larger for the general real VEV configuration h_6 than those of Figure 5.2. One can also observe that, when θ_{12} agrees with the data, θ_{13} is too large. Therefore, we are still not able to find a region of the parameter space where all three mixing angles are within experimental bounds. Thus, no real VEV of the type h_6 can reproduce current experimental data for the three mixing angles and the ratio R.

For the general complex VEV h_7, the R condition spans the full θ_{ij} parameter space nearly homogeneously. For this reason, in Figure 5.4, we have singled out the results which agree with experimental observations for s^2_{12}, s^2_{23}, making it clear that, in some of these cases, s^2_{13} is also within experimental bounds. Thus, a complex VEV can lead to valid results for θ_{ij} and R, so that we are interested in the VEV configurations of the softly-broken potential $V_{\text{SB}}(\Phi)$ with complex components. Details about the minimization of $V_{\text{SB}}(\Phi)$ are given in Appendix A.

Considering the general VEV configuration h_7 given in (5.13), it is clear that, if either of the parameters $\varepsilon_{1,2} = 0$, the charged-lepton mass matrix of (5.6) is singular, with at least one zero eigenvalue. Thus, this possibility is discarded, and of the VEVs determined in Appendix A, those of interest are the ones with $\theta_{1,2}, \varepsilon_{1,2} \neq 0$, corresponding to

$$\begin{aligned} h_8 &= v\left(1, \pm\varepsilon e^{i\theta}, \pm\varepsilon e^{-i\theta}\right) \quad , \quad \varepsilon^2 = \frac{\sin(\alpha+2\theta)}{\sin(\alpha-4\theta)}\,, \\ h_9 &= v\left(1, \pm\varepsilon_1 e^{i\theta_1}, \pm\varepsilon_2 e^{i\theta_2}\right) \quad , \quad \varepsilon_1^2 = \frac{\sin(\alpha-2\theta_2)}{\sin(\alpha-2\theta_1+2\theta_2)}\ ,\ \varepsilon_2^2 = \frac{\sin(\alpha+2\theta_1)}{\sin(\alpha-2\theta_1+2\theta_2)}\,, \end{aligned} \tag{5.16}$$

with $\alpha = \arg(\lambda'_4)$ [see (4.9)], $\theta \in [-\pi, \pi]$, and $\theta_{1,2} \in [-\pi, \pi]$. Notice that h_9 is under the additional condition

$$\lambda_4 = \frac{(3\lambda_2 - \lambda_3)\cos(\alpha+\theta_1-\theta_2)}{\cos(2\alpha-\theta_1+\theta_2)}\,, \tag{5.17}$$

implying fine-tuning among the parameters of the scalar potential. We have now inserted the above conditions in our code. The results for the mixing are presented in Figures 5.5 and 5.6 for h_8 and h_9, respectively. When compared to the general case presented in Figure 5.4, one can observe the presence of correlations within the angular distributions, rather than the more homogeneous patterns obtained for h_7. These correlations are more pronounced for h_8, where $\theta_2 = -\theta_1$ and λ_4 is free, suggesting that the parameters of the VEV configuration affect the angular results more directly than the parameters of the scalar potential. For both VEV configurations, we obtain cases where all three mixing angles, as well as R, are within the 3σ allowed range.

5.3 Scalar mass matrices

As was mentioned in the previous section, we have not been considering the regions of validity of each of the VEV configurations under analysis. Instead, the program sweeps the entire parameter space of

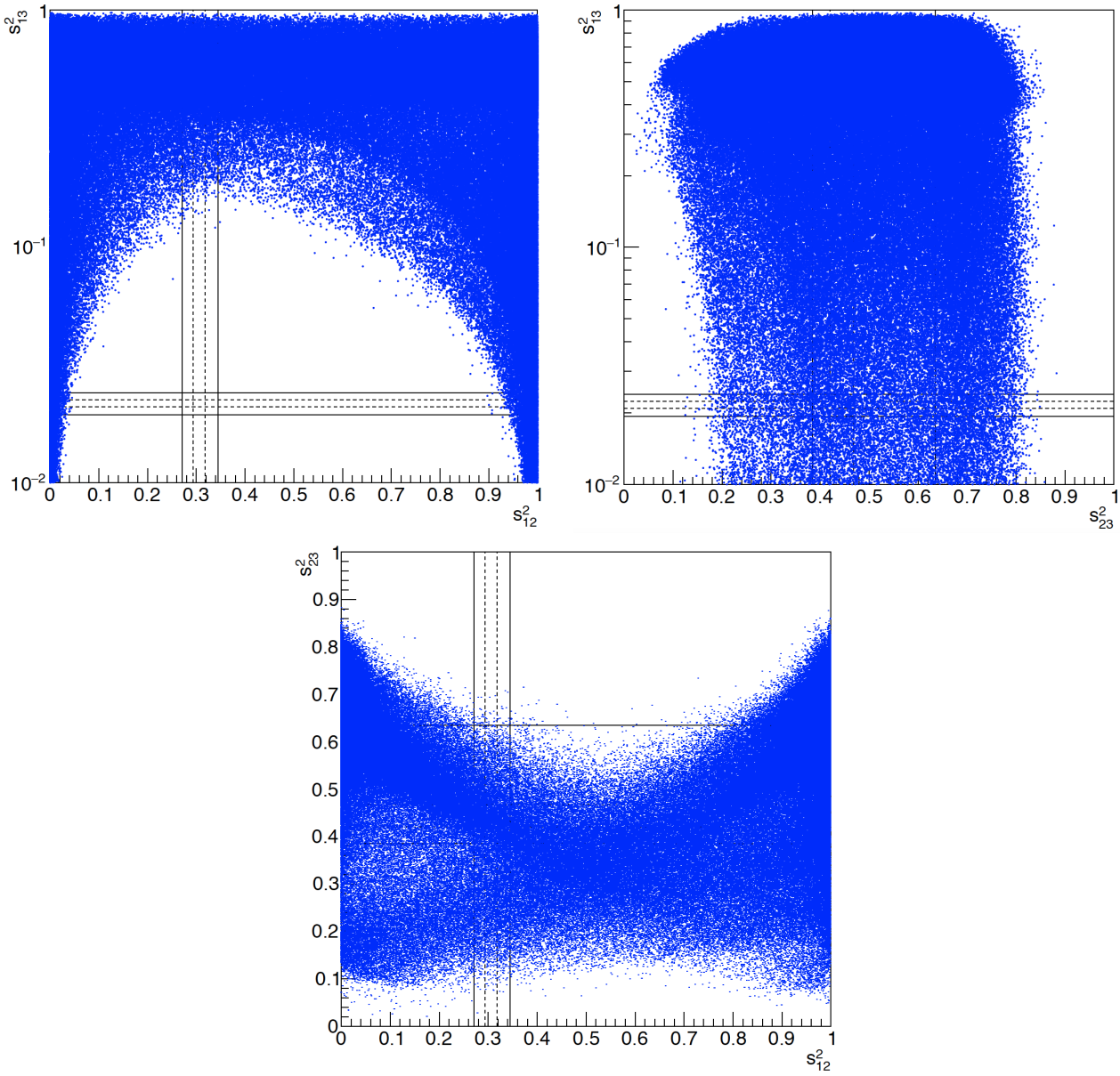

Figure 5.3: Values obtained for s^2_{ij} after RGE running of κ^{ij} and using h_6 for $\langle\Phi\rangle$. The axis corresponding to s^2_{13} is in logarithmic scale. The solid (dashed) black lines enclose the 3σ (1σ) allowed interval for each variable. In all cases R is within the 3σ experimental range.

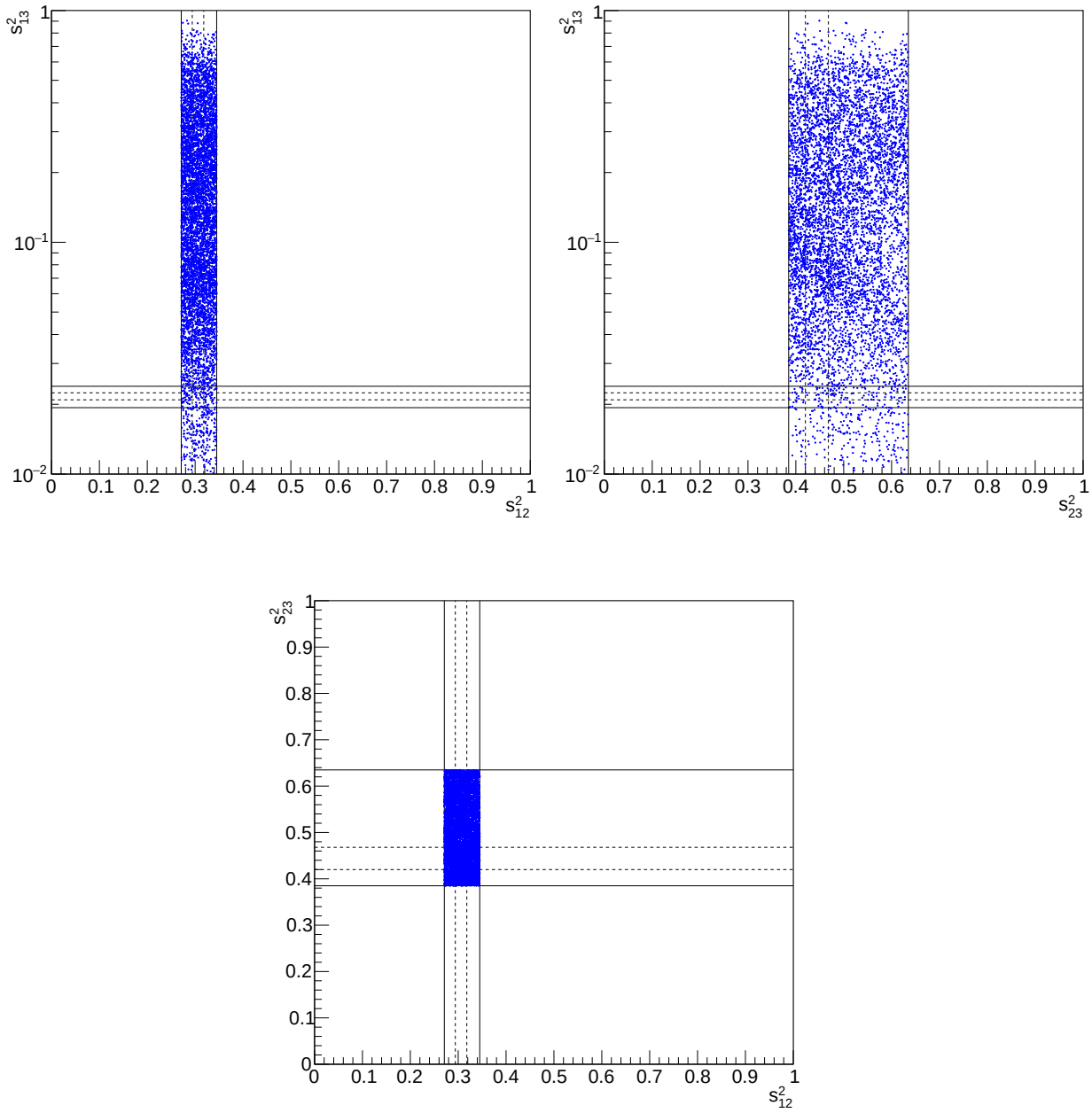

Figure 5.4: Values obtained for s^2_{ij} after RGE running of κ^{ij} and using h_τ for $\langle\Phi\rangle$. The axis corresponding to s^2_{13} is in logarithmic scale. The solid (dashed) black lines enclose the 3σ (1σ) allowed interval for each variable. In all cases R is within the 3σ experimental range.

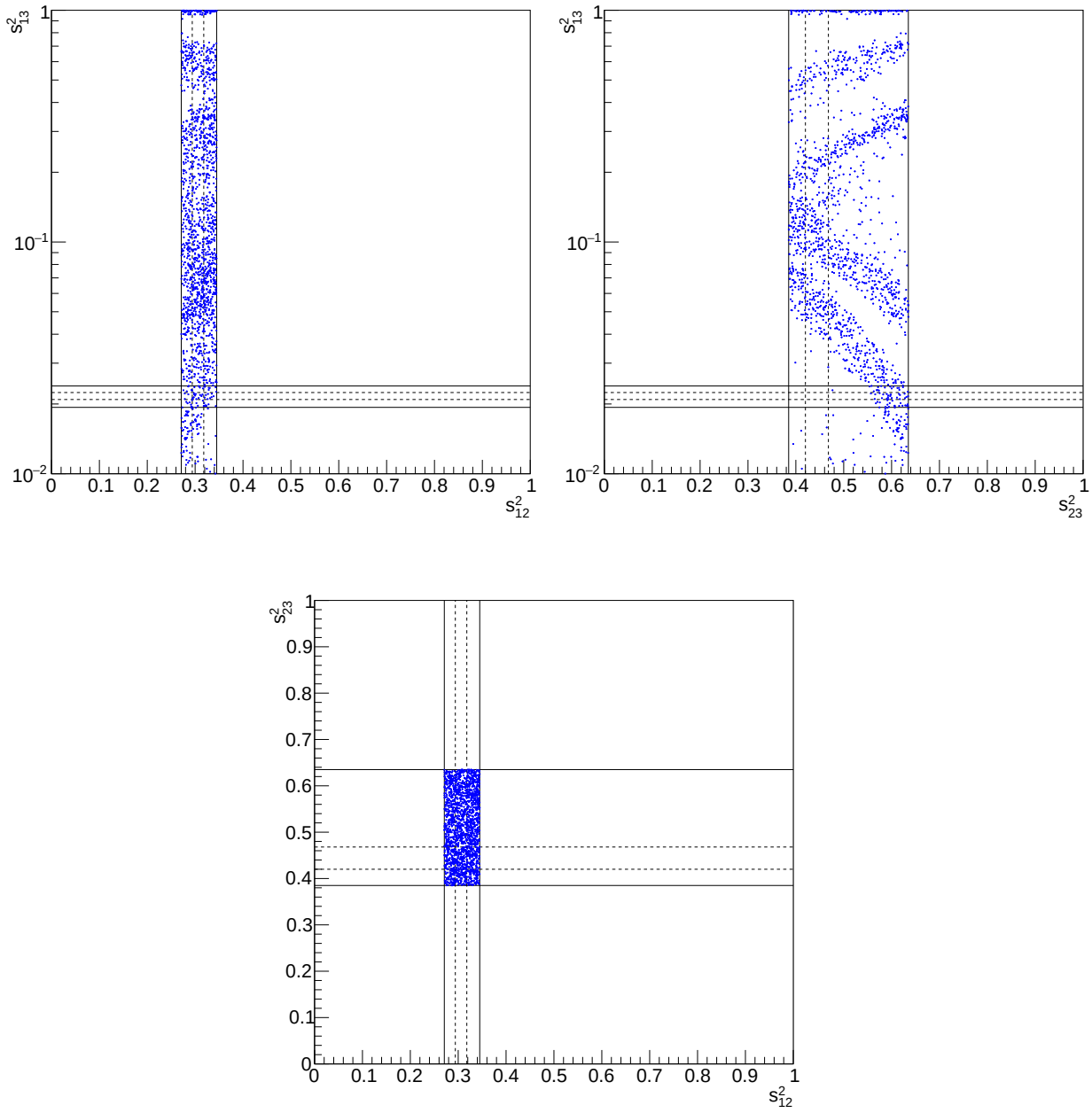

Figure 5.5: Values obtained for s^2_{ij} after RGE running of κ^{ij} and using h_8 for $\langle\Phi\rangle$. The axis corresponding to s^2_{13} is in logarithmic scale. The solid (dashed) black lines enclose the 3σ (1σ) allowed interval for each variable. In all cases $R,\ s^2_{12}\ s^2_{23}$ are within the 3σ experimental range.

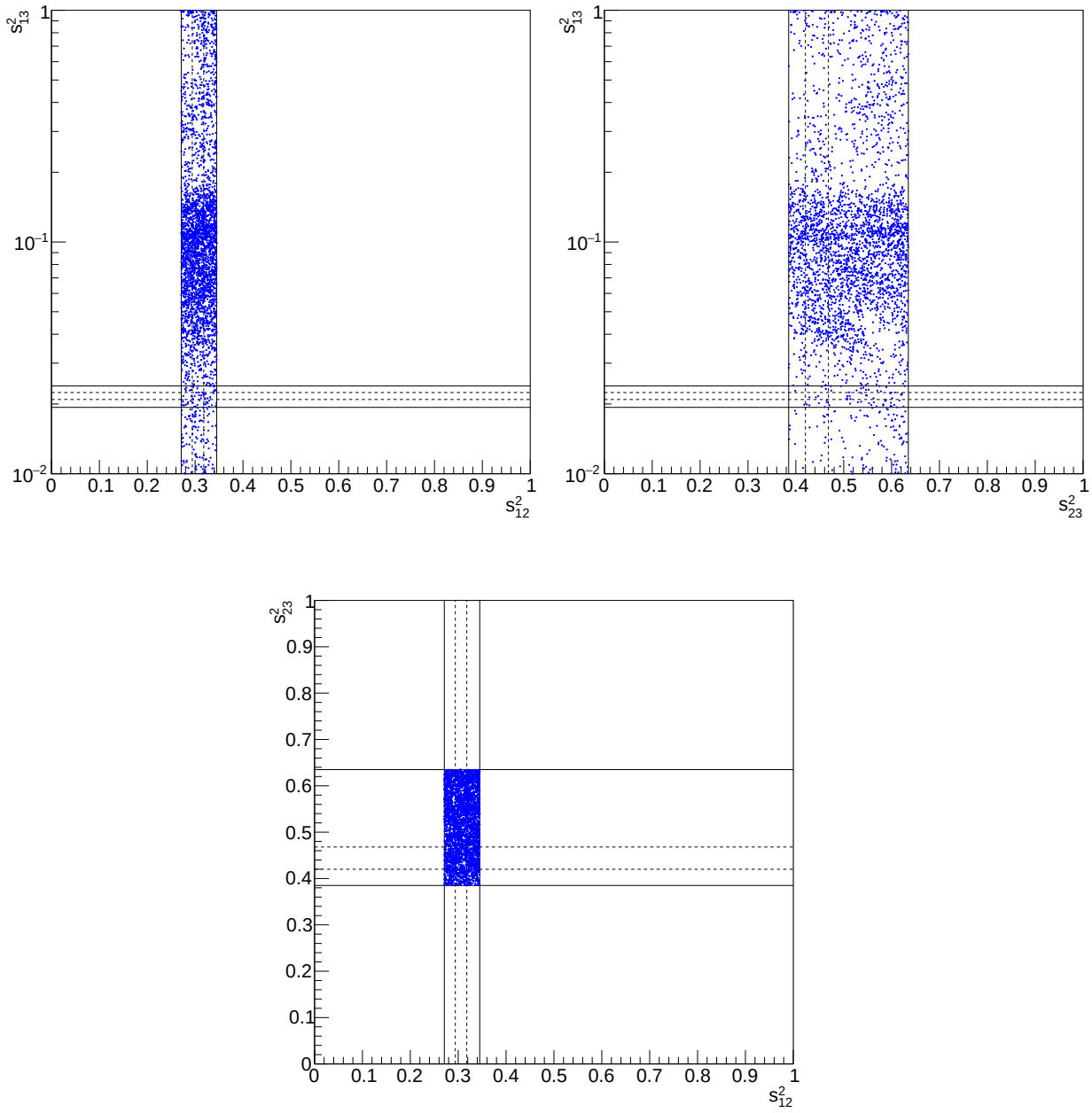

Figure 5.6: Values obtained for s^2_{ij} after RGE running of κ^{ij} and using h_9 for $\langle\Phi\rangle$. The axis corresponding to s^2_{13} is in logarithmic scale. The solid (dashed) black lines enclose the 3σ (1σ) allowed interval for each variable. In all cases $R,\ s^2_{12},\ s^2_{23}$ are within the 3σ experimental range.

the scalar Higgs potential, considering only $|\lambda_i| < 1$ $(i = 1, 2, 3, 4)$. It is however necessary to test the stability of $V_{\mathsf{SB}}(\Phi)$ by studying the scalar mass spectrum.

The mass matrices for the neutral and charged scalars, $\mathbf{M}_n$ and $\mathbf{M}_c$, respectively, are obtained from the scalar potential $V_{\mathsf{SB}}(\Phi)$ by

$$\begin{aligned}
(M_n)_{ij} &= \frac{1}{2}\left.\frac{\partial^2 V_{\mathsf{SB}}(\Phi)}{\partial\chi_i^0\partial\chi_j^0}\right|_{\langle\Phi\rangle} \quad , \quad \chi_i^0 = (\phi_{1\mathsf{R}}^0, \phi_{2\mathsf{R}}^0, \phi_{3\mathsf{R}}^0, \phi_{1\mathsf{I}}^0, \phi_{2\mathsf{I}}^0, \phi_{3\mathsf{I}}^0)\,, \\
(M_c)_{ij} &= \frac{1}{2}\left.\frac{\partial^2 V_{\mathsf{SB}}(\Phi)}{\partial\chi_i^+\partial\chi_j^+}\right|_{\langle\Phi\rangle} \quad , \quad \chi_i^+ = (\phi_{1\mathsf{R}}^+, \phi_{2\mathsf{R}}^+, \phi_{3\mathsf{R}}^+, \phi_{1\mathsf{I}}^+, \phi_{2\mathsf{I}}^+, \phi_{3\mathsf{I}}^+)\,,
\end{aligned} \tag{5.18}$$

where χ_i^0 refers to the real and imaginary neutral fields of each of the three Higgs doublets, and χ_i^+ to the real and imaginary charged fields. Note that $\langle\chi_i^+\rangle = 0$. Thus, an extreme of the potential, identified through the minimization procedure discussed in Appendix A, is a true minimum, rather than a maximum or saddle point, when all eigenvalues of the mass matrices are nonnegative. We can set a test for the validity of the VEV configurations in our program by studying the sign of the eigenvalues of $\mathbf{M}_n$ and $\mathbf{M}_c$.

With the determination of the scalar mass matrices, we can obtain the masses of the scalars of our model, given that the eigenvalues of the matrices are the squared scalar masses. This introduces an additional constraint, related to the Higgs boson. It is known that the LHC has detected a neutral boson [32] of mass

$$m_{\mathsf{H}^0} = 125 \pm 0.24 \text{ GeV}\,, \tag{5.19}$$

which corresponds to the Higgs boson of the SM. As our model has an extended scalar sector, the number of massive neutral bosons is increased from one to five, so that it is expected that the lightest neutral boson of the model should have a mass compatible with m_{H^0}. This additional constraint must be taken into account when determining the validity of the model.

We have obtained the scalar mass matrices through (5.18) but, due to their large dimension, as each is a 6×6 matrix, we are not capable of determining the eigenvalues analytically. Instead, we input the mass matrices into our numerical code, which performs their diagonalization in order to determine the eigenvalues numerically, for each point generated in the parameter space of $V_{\mathsf{SB}}(\Phi)$. Given the large dimension of this space, which the program samples randomly, it should not be a trivial task to find points within the experimental 3σ allowed range for all mixing parameters where all eigenvalues of the scalar mass matrices are nonnegative. Thus, we alter the code so that it performs a fit of the model to the available experimental data, corresponding to the three lepton mixing angles, the ratio R of (4.48) and the Higgs mass m_{H^0}, under the constraint of real scalar masses, using as initial conditions points generated randomly in the parameter space of $V_{\mathsf{SB}}(\Phi)$. After this change, we run the program for the case corresponding to the VEV h_8. We find that the χ^2 of the fits never falls below ~ 100, indicating some difficulty with finding a point in the parameter space which can simultaneously lead to valid results for the neutrino parameters and for the observed Higgs mass. In order to explore this issue, we perform fits removing some of the constraints. In Figure 5.7 (5.8) are the results obtained without the constraint on the Higgs mass (the lepton mixing angles θ_{ij}). In both of these cases, we obtain several points where

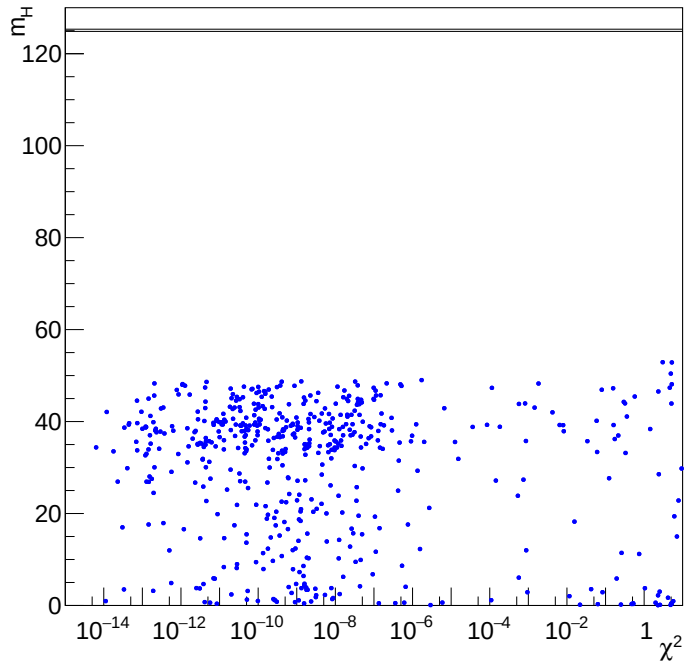

Figure 5.7: Values obtained for m_{H^0} as a function of χ^2 (scattered points) using h_8. All neutrino parameters are within the experimental 3σ allowed range. The full black lines enclose the 1σ allowed interval for m_{H^0}.

all constrained parameters are within their 3σ allowed range, with a corresponding $\chi^2 \sim 1$ or smaller.

From the results obtained, we can conclude that our model is capable of delivering either valid mixing angles or a valid Higgs boson mass, but not both. Rather, the region of the parameter space corresponding to a valid VEV configuration and to lepton mixing data within the experimental 3σ allowed range corresponds to a lightest neutral scalar which is too light, as its mass is never larger than 60 GeV (see Figure 5.7). Using the VEV h_9, for the case of fine tuning [see (5.17)], we obtain similar results and once more the Higgs mass m_{H^0} is not reproduced in the cases where the mixing angle constraints are in effect. This indicates that, with the VEV configurations available for $V_{\mathsf{SB}}(\Phi)$, we are not able to reproduce all experimental results. However, as this is due to the fact that we can obtain valid results for each observable individually, but not all observables simultaneously, the issue seems to lie with the incompatibility of the region of validity of each observable. Thus, given a different potential with a different VEV configuration, these regions of validity would change, and it is possible that they could overlap in some way. In particular, the soft-breaking term considered in Section 5.1 is not unique, since it was obtained for $\langle\Psi\rangle \sim (1,0,0)$. By choosing a different $\langle\Psi\rangle$, from those given in (4.10), we obtain a different soft-breaking term.

As an example, let us take $\langle\Psi\rangle \sim (1,1,0)$, obtained from $h_4 = v(1,e^{i\alpha_4},0)$ by setting $\alpha_4 = 0$. With such a VEV, both singlet and triplet interactions of $(\Phi^\dagger\Phi)$ and $(\Psi^\dagger\Psi)$ survive upon SSB of Ψ. Thus, two distinct terms are added to the potential $V(\Phi)$, in such a way that

$$V_{\mathsf{SB},4}(\Phi) = V(\Phi) + M_4^2\left(\phi_1^\dagger\phi_1 + \phi_2^\dagger\phi_2 - 2\phi_3^\dagger\phi_3\right) + M_\alpha^2\left(\phi_2^\dagger\phi_1 + \mathsf{H.c.}\right) . \tag{5.20}$$

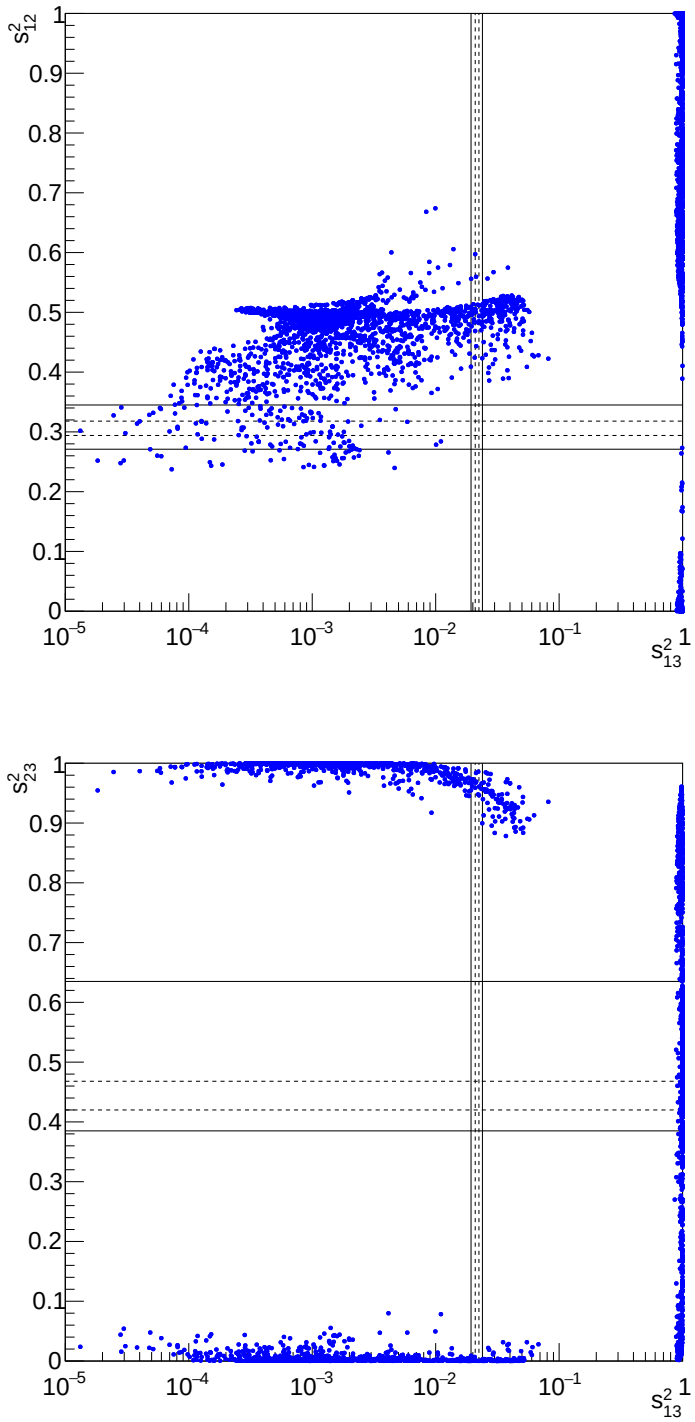

Figure 5.8: Values obtained for s^2_{ij} after RGE running of κ^{ij} and using h_8 for $\langle\Phi\rangle$. The axis corresponding to s^2_{13} is in logarithmic scale. The solid (dashed) black lines enclose the 3σ (1σ) allowed interval for each variable. In all cases $R,\ m_{\mathrm{H}^0}$ are within the 3σ experimental range.

Following a procedure similar to the one outlined in Appendix A, we obtain the minimization equations for $V_{\mathsf{SB},4}(\Phi)$. Focusing on the general case $v(1, \varepsilon_1 e^{i\theta_1}, \varepsilon_2 e^{i\theta_2})$, with $\varepsilon_{1,2} \neq 0$, we use three of the equations to obtain expressions for m^2, M_4^2, and M_α^2, and replace them in the remaining equations, which are solved simultaneously by the conditions

$$\begin{aligned} \varepsilon_1^2 &= \frac{\sin(\alpha - 2\theta_2)}{\sin(\alpha - 2\theta_1 + 2\theta_2)}\,, \\ \varepsilon_2^2 &= \frac{\cos(\alpha - \theta_1)\sin(\alpha - 2\theta_2)\sin(\theta_1 - 2\theta_2)\left[(3\lambda_2 - \lambda_3)\cos\theta_1 + \lambda_4 \sin(\alpha + \theta_1)\cot\theta_1\right]}{\lambda_4 \cos\alpha \sin(\alpha - 2\theta_2)\sin(\theta_1 - 2\theta_2)\sin(\alpha - 2\theta_1 + 2\theta_2)\cot\theta_1}\,, \end{aligned} \tag{5.21}$$

leaving $\theta_{1,2}$ free. For his new VEV configuration we compute the scalar mass matrices obtained from the potential $V_{\mathsf{SB},4}(\Phi)$, and change the program accordingly. We find results quite similar to those obtained with h_8, where the points with valid lepton mixing parameters are associated with a too light Higgs. This leads to the conclusion that this VEV configuration, as well, cannot reproduce data and the right value for the Higgs.

Chapter 6

Conclusions

In this thesis, we investigated a key topic of study in modern particle physics: the existence of neutrino masses, which are unaccounted for in the current model for the description of elementary particles, the SM. We began by introducing in Chapter 2 the SM in its current formulation. Then, we presented in the following chapter some extensions of the SM which, by including additional degrees of freedom, give rise to neutrino masses. We then moved on to a description and study of the model introduced in this thesis, in Chapter 4. We extended the SM with a single RH neutrino and three Higgs doublets instead of one, and applied an additional constraint by imposing invariance under the discrete group A_4. The A_4-symmetric scalar potential and the resulting VEV configurations were presented in Section 4.2. Using these, we determined the neutrino mass matrix at the very large energy scale M_R of operation of the seesaw mechanism that gives rise to neutrino masses, given by (4.23). Afterwards, the RGE of the flavor coupling matrices κ^{ij} were used to obtain the masses at the energy scale of current experiments. After a numerical analysis of the RGE using a leading-log approximation, described in Section 4.6, we concluded that the model could not reproduce experimental results for neutrino mass-squared differences, as it was not possible to lift the degeneracy between neutrino masses, obtaining for the ratio R, defined in (4.48), a value smaller than experimental prediction by around ten orders of magnitude and, given the limited precision of the method used, compatible with zero. These results suggest that the observed degeneracy is protected by the imposed A_4 symmetry, which is not broken at the M_R scale but rather at the scale of EWSB where the neutrinos obtain mass, so that the effects of the RGE are constrained by the effect of this symmetry. Thus, if it were possible to break the A_4 symmetry at the M_R scale, it was expected that the neutrino mass-squared differences would take on a much wider range of values.

Given these conclusions, we considered in Chapter 5 an alteration to our model, consisting of an additional term in the Lagrangian which is not invariant under A_4, so that the symmetry is softly broken. We concluded that the soft-breaking must be performed in the scalar sector, by the addition of an A_4 triplet of scalar singlet fields Ψ which would interact with the Higgs fields, as described in Section 5.1. This gives rise to a distinct scalar potential $V_{\text{SB}}(\Phi)$ upon SSB, given by (5.4), with a different set of VEV configurations to the A_4-symmetric potential, as explored in Appendix A. The new neutrino mass matrix

was obtained and the RGE running resulted in a wide range of results, presented in Figure 5.1, including several cases in which the mass-squared difference ratio R is within experimental bounds.

We moved on to the study of the neutrino mixing angles, which are also restricted by experimental observations. For the VEV configuration we had been considering, the results were not in agreement with experimental observations, as presented in Figure 5.2, and we reached the eventual conclusion that no valid results can be obtained using a real VEV, as illustrated in Figure 5.3, obtained using a general real VEV configuration h_6, defined in (5.12). On the other hand, using a general complex VEV configuration h_7, defined in (5.13), it was possible to find cases in agreement with experimental results, as shown in Figure 5.4. In fact, it can be seen that, even allowing full freedom to all parameters of h_6 (apart from the normalization v, of course), the resulting distribution for the mixing angles, under the condition that R is within the experimental 3σ allowed range, is restricted to specific areas of the parameter space, which do not contain the region where all mixing angles are compatible with experimental results. In the case of h_7, this is not verified, and the experimental 3σ allowed ranges for the mixing angles are well populated. Thus, we concluded that complex phases in the Higgs VEV are essential for the reproduction of experimental results of the lepton mixing angles, and continued our analysis using the complex VEVs $h_{8,9}$ given by (**??**) and (**??**) respectively. We found valid results for both configurations, as presented in Figures 5.5 and 5.6, where we can observe, especially for h_8, that the data points which are in agreement with experimental observations for s^2_{12}, s^2_{23} are distributed in a specific pattern in the plots including s^2_{13}, suggesting the existence of relations between the mixing angles.

We were left with the requirement of verifying the validity of the VEV configurations used, using the scalar mass matrices defined in (5.18). Under the condition that all eigenvalues of these matrices must be nonnegative, we fitted the model to the constraints given by experimental observations of the lepton mixing angles θ_{ij}, the ratio R, and the scalar boson mass m_{H^0}. It was determined that it is not possible to obtain cases where all constraints are simultaneously satisfied but, by removing different constraints in turn, all can be satisfied individually, as it is clear in Figures 5.8 and 5.7. Thus, if one could find a case where the conditions for satisfying all constraints overlap, the model would provide valid results. To pursue this idea, we considered a different scalar potential, obtained by taking an alternative VEV configuration for the scalar triplet Ψ. This generated a different VEV configuration for Φ and different scalar mass matrices. However, this alternative led to similar results, with a scalar mass spectrum that is too light.

6.1 Future work and achievements

Based on the results obtained, the logical conclusion is that the model analyzed in this thesis is not capable of reproducing both neutrino and Higgs results. However, some possibilities of alteration of our model remain, due to the different avenues of A_4 soft breaking which are yet to be explored. The soft breaking is performed with the scalar singlet fields Φ, under the assumption that $\langle\Phi\rangle \sim (1,0,0)$, initially, and that $\langle\Phi\rangle \sim (1,1,0)$, in a subsequent analysis, leaving unexplored the cases where Φ takes one of the remaining VEV configurations of (4.10). As mentioned in Section 5.3, each of the four VEV

configurations h_i leads to a distinct potential $V_{\text{SB},i}(\phi)$, according to

$$\begin{aligned}
h_2 &\to V_{\text{SB},2}(\phi) = V(\phi) + M_2^2 \left(\phi_2^\dagger \phi_3 + \phi_3^\dagger \phi_1 + \phi_1^\dagger \phi_2 + \text{H.c.}\right), \\
h_3 &\to V_{\text{SB},3}(\phi) = V(\phi) + M_3^2 \left[\omega \left(\phi_2^\dagger \phi_3 - \phi_3^\dagger \phi_1 - \phi_1^\dagger \phi_2\right) + \text{H.c.}\right], \\
h_4 &\to V_{\text{SB},4}(\phi) = V(\phi) + M_4^2 \left(\phi_1^\dagger \phi_1 + \phi_2^\dagger \phi_2 - 2\phi_3^\dagger \phi_3\right) + M_\alpha^2 \left(e^{i\alpha_4} \phi_2^\dagger \phi_1 + \text{H.c.}\right),
\end{aligned} \tag{6.1}$$

with $V_{\text{SB},1} \equiv V_{\text{SB}}$ as defined in (5.4). Each of the these scalar potentials will have distinct VEV configurations with their own regions of validity, along with distinct scalar mass matrices, altering the results of the model. Hopefully, among the possibilities (6.1), one (or more) will lead to valid results for the model. Thus, it is necessary to fully explore all these possibilities before making final conclusions on the validity of the model.

With this thesis, we have considered a popular discrete symmetry based on the A_4 group, and explored a less typical avenue by focusing on enlarging the scalar sector rather than the fermionic one. This led to the study of a previously unconsidered model, which was found to be compatible with neutrino data but hard to reconcile with Higgs mass results. Still, there are unexplored possibilities to consider, leaving open a window for further work on the subject. The focus on the A_4 group was motivated by its ideal set of representations, as aforementioned. However, there are other discrete groups with appropriate representations, such as the group S_4, which could also be considered as an imposed symmetry for a single right-handed neutrino model. As A_4 is a subgroup of S_4, the results obtained should be similar, but perhaps different enough to provide valid results, so that this is another venue to be considered.

Finally, some additional issues could be further explored with a more in-depth analysis in a framework compatible with both neutrino and Higgs results. For instance, the study of the quark sector will have rich phenomenology in the case where the three Higgs doublets of the theory couple to quarks. In a more advanced phase, these results, along with the scalar mass spectrum, could be used to further validate the model and provide experimental evidence of new physics.

Bibliography

[1] S. L. Glashow, *Nucl. Phys.* **22**, 579 (1961).

[2] M. Gell-Mann, *Phys. Lett.* **8**, 214 (1964).

[3] G. Zweig, An SU(3) Model for Strong Interaction Symmetry and its Breaking, *CERN Report No.8182/TH.401* (1964).

[4] S. Weinberg, *Phys. Rev. Lett.* **19**, 1264 (1967).

[5] A. Salam, *8th Nobel Symposium* (1968), p. 367.

[6] F. Englert, R. Brout, *Phys. Rev. Lett.* **13**, 321 (1964).

[7] P. W. Higgs, *Phys. Rev. Lett.* **13**, 508 (1964).

[8] G. S. Guralnik, C. R. Hagen, T. W. B. Kibble, *Phys. Rev. Lett.* **13**, 585 (1964).

[9] F. J. Hasert, *et al.* (Gargamelle Neutrino Collaboration), *Phys. Lett. B* **46**, 121 (1973).

[10] F. J. Hasert, *et al.* (Gargamelle Neutrino Collaboration), *Phys. Lett. B* **46**, 138 (1973).

[11] F. J. Hasert, *et al.* (Gargamelle Neutrino Collaboration), *Nucl. Phys. B* **73**, 1 (1974).

[12] G. Arnison, *et al.* (UA1 Collaboration), *Phys. Lett. B* **122**, 103 (1983).

[13] M. Banner, *et al.* (UA2 Collaboration), *Phys. Lett. B* **122**, 476 (1983).

[14] G. Arnison, *et al.* (UA1 Collaboration), *Phys. Lett. B* **126**, 398 (1983).

[15] P. Bagnaia, *et al.* (UA2 Collaboration), *Phys. Lett. B* **129**, 130 (1983).

[16] G. Aad, *et al.* (ATLAS Collaboration), *Phys. Lett. B* **716**, 1 (2012).

[17] S. Chatrchyan, *et al.* (CMS Collaboration), *Phys. Lett. B* **716**, 30 (2012).

[18] J. Chadwick, *Verh. d Phys. Ges.* **16**, 383 (1914).

[19] E. Fermi, *Zeitschrift für Physik* **88**, 161 (1934).

[20] C. L. Cowan, *et al.*, *Science* **124**, 103 (1956).

[21] G. Danby, *et al.*, *Phys. Rev. Lett.* **9**, 36 (1962).

[22] K. Kodama, *et al.* (Donut Collaboration), *Phys. Lett. B* **504**, 218 (2001).

[23] R. Davis, D. S. Harmer, K. C. Hoffman, *Phys. Rev. Lett.* **20**, 1205 (1968).

[24] B. Pontecorvo, *Zh. Eksp. Teor. Fiz.* **33**, 549 (1957).

[25] Q. R. Ahmad, *et al.* (SNO Collaboration), *Phys. Rev. Lett.* **87**, 071301 (2001).

[26] M. Peskin, D. Schroeder, *An Introduction to Quantum Field Theory* (Westview Press, 1995).

[27] N. Cabibbo, *Phys. Rev. Lett.* **10**, 531 (1963).

[28] M. Kobayashi, T. Maskawa, *Prog. Theor. Phys.* **49**, 652 (1973).

[29] L. L. Chau, W. Y. Keung, *Phys. Rev. Lett.* **53**, 1802 (1984).

[30] C. Wu, *et al.*, *Phys. Rev.* **105**, 1413 (1957).

[31] I. Esteban, *et al.*, *JHEP* **01**, 87 (2017).

[32] C. Patrignani, *et al.* (Particle Data Group), *Chin. Phys. C* **40**, 100001 (2016).

[33] C. Giunti, C. W. Kim, *Fundamentals of Neutrino Physics and Astrophysics* (Oxford University Press, 2007).

[34] S. Weinberg, *Phys. Rev. Lett.* **43**, 1566 (1979).

[35] B. Pontecorvo, *Zh. Eksp. Teor. Fiz.* **34**, 247 (1957).

[36] Z. Maki, M. Nakagawa, S. Sakata, *Prog. Theor. Phys.* **28**, 870 (1962).

[37] F. Capozzi, *et al.*, *Nucl. Phys. B* **908**, 218 (2016).

[38] D. V. Forero, M. Tortola, J. W. F. Valle, *Phys. Rev. D* **90**, 093006 (2014).

[39] P. Minkowski, *Phys. Lett. B* **67**, 421 (1977).

[40] T. Yanagida, *Proc. of the Workshop on Unified Theory and Baryon Number in the Universe*, O. Sawada, A. Sugamoto, eds. (1979).

[41] S. L. Glashow, *Quarks and Leptons* (Cargèse, 1980), chap. 15, p. 687.

[42] M. Gell-Mann, P. Ramon, R. Slansky, *Supergravity* (North-Holland Publishing Company, 1979).

[43] R. N. Mohapatra, G. Senjanovic, *Phys. Rev. Lett.* **44**, 912 (1980).

[44] R. Foot, H. Lew, X. G. He, G. C. Joshi, *Z. Phys. C* **44**, 441 (1989).

[45] W. Konetschny, W. Kummer, *Phys. Lett. B* **70**, 433 (1977).

[46] T. P. Cheng, L. F. Li, *Phys. Rev. D* **22**, 2860 (1980).

[47] J. Schechter, J. W. F. Valle, *Phys. Rev. D* **22**, 2227 (1980).

[48] G. Lazarides, Q. Shafi, C. Wetterich, *Nucl. Phys. B* **181**, 287 (1981).

[49] W. Grimus, L. Lavoura, *Eur. Phys. J. C* **39**, 219 (2005).

[50] S. F. King, C. Luhn, *Rept. Prog. Phys.* **76**, 056201 (2013).

[51] W. K. Tung, *Group Theory in Physics* (World Scientific Publishing Company, 1985).

[52] J. Barry, W. Rodejohann, *Phys. Rev. D* **81**, 093002 (2010).

[53] E. Ma, G. Rajasekaran, *Phys. Rev. D* **64**, 113012 (2001).

[54] A. Degee, I. P. Ivanov, V. Keus, *JHEP* **02**, 125 (2013).

[55] R. G. Felipe, H. Serôdio, J. P. Silva, *Phys. Rev. D* **88**, 015015 (2013).

[56] J. Heeck, *et al.*, *Nucl. Phys. B* **896**, 281 (2015).

[57] S. Antusch, J. Kersten, M. Lindner, M. Ratz, *Nucl. Phys. B* **674**, 401 (2003).

Appendix A

Minimization of the softly-broken Higgs potential

We recall that the charged field of each Higgs doublet must have a zero VEV and thus define

$$\langle \phi_a \rangle = \begin{pmatrix} \langle \phi_a^+ \rangle \\ \langle \phi_a^0 \rangle \end{pmatrix} = \frac{1}{\sqrt{2}} \begin{pmatrix} 0 \\ \langle \phi_{a\mathsf{R}}^0 \rangle + i \langle \phi_{a\mathsf{I}}^0 \rangle \end{pmatrix} , \tag{A.1}$$

where ϕ_a, $a = 1, 2, 3$, are the three Higgs doublets. We further define

$$\begin{gathered} \langle \phi_{a\mathsf{R}}^0 \rangle = \frac{v_a \cos\theta_a}{\sqrt{2}} \ , \ \langle \phi_{a\mathsf{I}}^0 \rangle = \frac{v_a \sin\theta_a}{\sqrt{2}} \, , \\ v_1 = v \ , \ v_2 = v\varepsilon_1 \ , \ v_3 = v\varepsilon_2 \ , \ \theta_1 = 0 \, , \end{gathered} \tag{A.2}$$

so that we obtain the most general complex VEV configuration, $v/2(1, \varepsilon_1 e^{i\theta_1}, \varepsilon_2 e^{i\theta_2})$. We define $V_{\mathsf{SB}}(\Phi)$ according to (5.4) and obtain the minimization equations, given by

$$\left. \frac{dV_{\mathsf{SB}}(\Phi)}{d\phi_{a\mathsf{R}}^0} \right|_{\langle \phi_a \rangle} = 0 \ , \ \left. \frac{dV_{\mathsf{SB}}(\Phi)}{d\phi_{a\mathsf{I}}^0} \right|_{\langle \phi_a \rangle} = 0 \, , \tag{A.3}$$

which lead to

$$\begin{aligned} \frac{v^3}{4\sqrt{2}} \Bigg\{ \frac{4m^2 + 8M_S^2}{v^2} + \left(1 + \varepsilon_1^2 + \varepsilon_2^2\right) \lambda_1 + 2\lambda_2 - \left(\varepsilon_1^2 + \varepsilon_2^2\right) (\lambda_2 - \lambda_3) \\ + \lambda_4 \left[\varepsilon_1^2 \cos\left(\alpha + 2\theta_1\right) + \varepsilon_2^2 \cos\left(\alpha - 2\theta_2\right) \right] \Bigg\} = 0 \, , \end{aligned} \tag{A.4a}$$

$$\begin{aligned} \frac{v^3 \varepsilon_1}{4\sqrt{2}} \Bigg\{ \left[\frac{4m^2 - 4M_S^2}{v^2} + \left(1 + \varepsilon_1^2 + \varepsilon_2^2\right) \lambda_1 - \left(1 - 2\varepsilon_1^2 + \varepsilon_2^2\right) \lambda_2 + \lambda_3 + \varepsilon_2^2 \lambda_3 \right] \cos\theta_1 \\ + \lambda_4 \left[\cos\left(\alpha + \theta_1\right) + \varepsilon_2^2 \cos\left(\alpha - \theta_1 + 2\theta_2\right) \right] \Bigg\} = 0 \, , \end{aligned} \tag{A.4b}$$

$$\begin{aligned} \frac{v^3 \varepsilon_2}{4\sqrt{2}} \Bigg\{ \left[\frac{4m^2 - 4M_S^2}{v^2} + \left(1 + \varepsilon_1^2 + \varepsilon_2^2\right) \lambda_1 - \left(1 + \varepsilon_1^2 - 2\varepsilon_2^2\right) \lambda_2 + \lambda_3 + \varepsilon_1^2 \lambda_3 \right] \cos\theta_2 \\ + \lambda_4 \left[\cos\left(\alpha - \theta_2\right) + \varepsilon_1^2 \cos\left(\alpha - 2\theta_1 + \theta_2\right) \right] \Bigg\} = 0 \, , \end{aligned} \tag{A.4c}$$

$$\frac{v^3}{4\sqrt{2}}\lambda_4\left[\varepsilon_1^2\sin\left(\alpha+2\theta_1\right)-\varepsilon_2^2\sin\left(\alpha-2\theta_2\right)\right]=0\,, \tag{A.4d}$$

$$\begin{aligned}\frac{v^3\varepsilon_1}{4\sqrt{2}}\left\{\left[\frac{4m^2-4M_S^2}{v^2}+\left(1+\varepsilon_1^2+\varepsilon_2^2\right)\lambda_1-\left(1-2\varepsilon_1^2+\varepsilon_2^2\right)\lambda_2+\lambda_3+\varepsilon_2^2\lambda_3\right]\sin\theta_1\right.\\ \left.+\lambda_4\left[-\sin\left(\alpha+\theta_1\right)+\varepsilon_2^2\sin\left(\alpha-\theta_1+2\theta_2\right)\right]\right\}=0\,,\end{aligned} \tag{A.4e}$$

$$\begin{aligned}\frac{v^3\varepsilon_2}{4\sqrt{2}}\left\{\left[\frac{4m^2-4M_S^2}{v^2}+\left(1+\varepsilon_1^2+\varepsilon_2^2\right)\lambda_1-\left(1+\varepsilon_1^2-2\varepsilon_2^2\right)\lambda_2+\lambda_3+\varepsilon_1^2\lambda_3\right]\sin\theta_2\right.\\ \left.+\lambda_4\left[\sin\left(\alpha-\theta_2\right)-\varepsilon_1^2\sin\left(\alpha-2\theta_1+\theta_2\right)\right]\right\}=0\,.\end{aligned} \tag{A.4f}$$

The minimization equations can be solved considering $(\varepsilon_1=0,\varepsilon_2=0)$, $(\varepsilon_1\neq 0,\varepsilon_2=0)$ or $(\varepsilon_1\neq 0,\varepsilon_2\neq 0)$.

A.1 $\varepsilon_1=0,\varepsilon_2=0$

In this case, the VEV configuration takes the form $v/2(1,0,0)$, analogous to h_1. All but one of the minimization equations are automatically satisfied, while the remaining equation, (A.4a), takes the form

$$v\frac{4m^2+8M_S^2+v^2\left(\lambda_1+2\lambda_2\right)}{4\sqrt{2}}=0\,, \tag{A.5}$$

determining

$$v^2=-4\frac{m^2+2M_S^2}{\lambda_1+2\lambda_2}\,. \tag{A.6}$$

A.2 $\varepsilon_1\neq 0,\varepsilon_2=0$

In this case, the VEV configuration is given by $v/2(1,\varepsilon_1 e^{i\theta_1},0)$. Equations (A.4c) and (A.4f) are automatically satisfied, leaving

$$\frac{v^3}{4\sqrt{2}}\left[\frac{4m^2+8M_S^2}{v^2}+\left(1+\varepsilon_1^2\right)\lambda_1+2\lambda_2-\varepsilon_1^2\left(\lambda_2-\lambda_3\right)+\lambda_4\varepsilon_1^2\cos\left(\alpha+2\theta_1\right)\right]=0\,, \tag{A.7a}$$

$$\frac{v^3\varepsilon_1}{4\sqrt{2}}\left\{\left[\frac{4m^2-4M_S^2}{v^2}+\left(1+\varepsilon_1^2\right)\lambda_1-\left(1-2\varepsilon_1^2\right)\lambda_2+\lambda_3\right]\cos\theta_1+\lambda_4\cos\left(\alpha+\theta_1\right)\right\}=0\,, \tag{A.7b}$$

$$\frac{v^3}{4\sqrt{2}}\lambda_4\varepsilon_1^2\sin\left(\alpha+2\theta_1\right)=0\,, \tag{A.7c}$$

$$\frac{v^3\varepsilon_1}{4\sqrt{2}}\left\{\left[\frac{4m^2-4M_S^2}{v^2}+\left(1+\varepsilon_1^2\right)\lambda_1-\left(1-2\varepsilon_1^2\right)\lambda_2+\lambda_3\right]\sin\theta_1-\lambda_4\sin\left(\alpha+\theta_1\right)\right\}=0\,. \tag{A.7d}$$

From (A.7c), we determine that

$$\theta_1=\frac{n\pi-\alpha}{2}\equiv\theta_\alpha\ ,\ n\in\mathbb{Z}. \tag{A.8}$$

Replacing θ_1 in (A.7), we obtain, for even n,

$$\begin{aligned}
&\frac{v^3}{4\sqrt{2}}\left[\frac{4m^2+8M_S^2}{v^2}+\left(1+\varepsilon_1^2\right)\lambda_1+2\lambda_2-\varepsilon_1^2\left(\lambda_2-\lambda_3-\lambda_4\right)\right]=0\,,\\
&\frac{v^3\varepsilon_1}{4\sqrt{2}}\left[\frac{4m^2-4M_S^2}{v^2}+\left(1+\varepsilon_1^2\right)\lambda_1-\left(1-2\varepsilon_1^2\right)\lambda_2+\lambda_3+\lambda_4\right]\cos\left(\alpha/2\right)=0\,,\\
&\frac{v^3\varepsilon_1}{4\sqrt{2}}\left[\frac{4m^2-4M_S^2}{v^2}+\left(1+\varepsilon_1^2\right)\lambda_1-\left(1-2\varepsilon_1^2\right)\lambda_2+\lambda_3+\lambda_4\right]\sin\left(\alpha/2\right)=0\,.
\end{aligned}\tag{A.9}$$

The solution to these equations is of the form

$$\begin{aligned}
\varepsilon_1^2&=1-\frac{12M_S^2}{v^2\left(-3\lambda_2+\lambda_3+\lambda_4\right)}\equiv 1-\Delta_+\,,\\
v^2&=4\left[-\frac{m^2}{2\lambda_1+\lambda_2+\lambda_3+\lambda_4}-\frac{M_S^2\left(3\lambda_1+3\lambda_2+\lambda_3+\lambda_4\right)}{\left(3\lambda_2-\lambda_3-\lambda_4\right)\left(2\lambda_1+\lambda_2+\lambda_3+\lambda_4\right)}\right]\,.
\end{aligned}\tag{A.10}$$

For odd n, we obtain the equations

$$\begin{aligned}
&\frac{v^3}{4\sqrt{2}}\left[\frac{4m^2+8M_S^2}{v^2}+\left(1+\varepsilon_1^2\right)\lambda_1+2\lambda_2-\varepsilon_1^2\left(\lambda_2-\lambda_3+\lambda_4\right)\right]=0\,,\\
&\frac{v^3\varepsilon_1}{4\sqrt{2}}\left[\frac{4m^2-4M_S^2}{v^2}+\left(1+\varepsilon_1^2\right)\lambda_1-\left(1-2\varepsilon_1^2\right)\lambda_2+\lambda_3-\lambda_4\right]\sin\left(\alpha/2\right)=0\,,\\
&\frac{v^3\varepsilon_1}{4\sqrt{2}}\left[\frac{4m^2-4M_S^2}{v^2}+\left(1+\varepsilon_1^2\right)\lambda_1-\left(1-2\varepsilon_1^2\right)\lambda_2+\lambda_3-\lambda_4\right]\cos\left(\alpha/2\right)=0\,.
\end{aligned}\tag{A.11}$$

which, when solved, give

$$\begin{aligned}
\varepsilon_1^2&=1-\frac{12M_S^2}{v^2\left(-3\lambda_2+\lambda_3-\lambda_4\right)}\equiv 1-\Delta_-\,,\\
v^2&=4\left[-\frac{m^2}{2\lambda_1+\lambda_2+\lambda_3-\lambda_4}-\frac{M_S^2\left(3\lambda_1+3\lambda_2+\lambda_3-\lambda_4\right)}{\left(3\lambda_2-\lambda_3+\lambda_4\right)\left(2\lambda_1+\lambda_2+\lambda_3-\lambda_4\right)}\right]\,.
\end{aligned}\tag{A.12}$$

Thus, we obtain a VEV configuration of the form $v/2(1,\pm\sqrt{1-\Delta_\pm}e^{i\theta_\alpha},0)$, analogous to h_4. This includes the case $\theta_1=0$, for $\alpha=n\pi$.

A.3 $\varepsilon_1\neq 0, \varepsilon_2\neq 0$

Considering a general complex VEV configuration, we begin by using (A.4a) and (A.4c) to obtain expressions for m^2 and M_S^2, so that they can be replaced in the remaining equations, obtaining

$$\begin{aligned}
\frac{v^3\varepsilon_1}{4\sqrt{2}}\Big\{&\left[\left(\varepsilon_1^2-\varepsilon_2^2\right)\left(3\lambda_2-\lambda_3\right)-\varepsilon_1^2\lambda_4\cos\left(\alpha-2\theta_1+\theta_2\right)\sec\theta_2\right]\cos\theta_1\\
&+\lambda_4\left[\varepsilon_2^2\cos\left(\alpha-\theta_1+2\theta_2\right)-\sec\theta_2\sin\alpha\sin\left(\theta_1+\theta_2\right)\right]\Big\}=0\,,
\end{aligned}\tag{A.13a}$$

$$\frac{v^3}{4\sqrt{2}}\lambda_4\left[\varepsilon_1^2\sin\left(\alpha+2\theta_1\right)-\varepsilon_2^2\sin\left(\alpha-2\theta_2\right)\right]=0\,,\tag{A.13b}$$

$$\frac{v^3\varepsilon_1}{8\sqrt{2}}\left\{\left(\varepsilon_1^2-\varepsilon_2^2\right)\left[2\sin\theta_1\left(3\lambda_2-\lambda_3\right)-\lambda_4\sec\theta_2\sin\left(\alpha-\theta_1+\theta_2\right)\right]-4\lambda_4\cos\alpha\sin\theta_1\right.$$
$$\left.+\lambda_4\sec\theta_2\left[-2\cos\left(\theta_1-\theta_2\right)\sin\alpha+\varepsilon_1^2\sin\left(\alpha-3\theta_1+\theta_2\right)+\varepsilon_2^2\sin\left(\alpha-\theta_1+3\theta_2\right)\right]\right\}=0\,, \tag{A.13c}$$

$$\frac{v^3\varepsilon_2}{4\sqrt{2}}\lambda_4\left[\sin\left(\alpha-2\theta_2\right)-\varepsilon_1^2\sin\left(\alpha-2\theta_1+2\theta_2\right)\right]\sec\theta_2=0\,. \tag{A.13d}$$

We solve (A.13b) and (A.13d) for $\varepsilon_{1,2}$ and obtain

$$\varepsilon_1^2=\frac{\sin\left(\alpha-2\theta_2\right)}{\sin\left(\alpha-2\theta_1+2\theta_2\right)}\ ,\ \varepsilon_2^2=\frac{\sin\left(\alpha+2\theta_1\right)}{\sin\left(\alpha-2\theta_1+2\theta_2\right)}\,. \tag{A.14}$$

Replacing these results in (A.13), we are left with two equations,

$$\begin{aligned}&\frac{v^3\cos\theta_1\sqrt{\sin\left(\alpha-2\theta_2\right)}\sin\left(\theta_1+\theta_2\right)}{2\sqrt{2}\sin\left(\alpha-2\theta_1+2\theta_2\right)^{3/2}}\left[\left(-3\lambda_2+\lambda_3\right)\cos\left(\alpha+\theta_1-\theta_2\right)+\lambda_4\cos\left(2\alpha-\theta_1+\theta_2\right)\right]=0\,,\\&\frac{v^3\sin\theta_1\sqrt{\sin\left(\alpha-2\theta_2\right)}\sin\left(\theta_1+\theta_2\right)}{2\sqrt{2}\sin\left(\alpha-2\theta_1+2\theta_2\right)^{3/2}}\left[\left(-3\lambda_2+\lambda_3\right)\cos\left(\alpha+\theta_1-\theta_2\right)+\lambda_4\cos\left(2\alpha-\theta_1+\theta_2\right)\right]=0\,.\end{aligned} \tag{A.15}$$

We find all possible values of $\theta_{1,2}$ which satisfy these equations. Not considering the possibility of fine tuning of the parameters of the scalar potential, we find two solutions, given by

$$\theta_2=n\pi-\theta_1\ ,\ n\in\mathbb{Z}\,, \tag{A.16a}$$

$$\theta_2=\frac{m\pi-\alpha}{2}\ ,\ m\in\mathbb{Z}\,. \tag{A.16b}$$

We replace θ_2 in (A.14). For (A.16b), we obtain $\varepsilon_1=0$ and thus discard the possibility. This leaves us with (A.16a), which leads to

$$\varepsilon_1^2=\varepsilon_2^2=\frac{\sin\left(\alpha+2\theta_1\right)}{\sin\left(\alpha-4\theta_1\right)}\equiv\varepsilon^2\,. \tag{A.17}$$

Thus, we obtain a VEV configuration of the form $v/2\left(1,\pm\varepsilon e^{i\theta_1},\pm\varepsilon e^{-i\theta_1}\right)$. The expressions for v and θ_1 can be determined from those of m^2 and M_S^2, obtained from (A.4a) and (A.4c). However, we were not capable of inverting such complex trigonometric equations and thus we tentatively leave θ_1 free. As for v, we obtain

$$v^2=\frac{-12m^2}{3\lambda_1+2\lambda_3+\csc\left(\alpha-4\theta_1\right)\left\{2\lambda_4\sin\left(2\alpha-2\theta_1\right)+2\left[3\lambda_1+2\lambda_3+\lambda_4\cos\left(\alpha+2\theta_1\right)\right]\sin\left(\alpha+2\theta_1\right)\right\}}\,. \tag{A.18}$$

It is also possible to consider the case of fine tuning, in which we solve (A.15) for λ_4 and obtain

$$\lambda_4=\frac{\left(3\lambda_2-\lambda_3\right)\cos\left(\alpha+\theta_1-\theta_2\right)}{\cos\left(2\alpha-\theta_1+\theta_2\right)}\,. \tag{A.19}$$

This leaves both $\theta_{1,2}$ free, as the issue of the prior analysis remains, and introduces instead a restriction on the parameter space of the scalar potential. It is possible to determine v, but we obtain an unwieldy function of $\theta_{1,2}$ and the parameters of $V_{\text{SB}}(\Phi)$, which we skip for brevity.

Before moving on, we consider the cases where one or more complex phases are zero. Following a similar procedure to the one outlined above, we reach the conclusion that there are no solutions for

only one complex phase. When both phases are set to zero, there is a solution for $\alpha = 0$. Under these conditions, the equations (A.4) are given by

$$\frac{v^3}{4\sqrt{2}}\left[\frac{4m^2+8M_S^2}{v^2}+\left(1+\varepsilon_1^2+\varepsilon_2^2\right)\lambda_1+2\lambda_2-\left(\varepsilon_1^2+\varepsilon_2^2\right)\left(\lambda_2-\lambda_3-\lambda_4\right)\right]=0\,, \tag{A.20a}$$

$$\frac{v^3\varepsilon_1}{4\sqrt{2}}\left[\frac{4m^2-4M_S^2}{v^2}+\left(1+\varepsilon_1^2+\varepsilon_2^2\right)\lambda_1-\lambda_2+2\varepsilon_1^2\lambda_2+\lambda_3+\lambda_4+\varepsilon_2^2\left(-\lambda_2+\lambda_3+\lambda_4\right)\right]=0\,, \tag{A.20b}$$

$$\frac{v^3\varepsilon_2}{4\sqrt{2}}\left[\frac{4m^2-4M_S^2}{v^2}+\left(1+\varepsilon_1^2+\varepsilon_2^2\right)\lambda_1-\lambda_2+2\varepsilon_2^2\lambda_2+\lambda_3+\lambda_4+\varepsilon_1^2\left(-\lambda_2+\lambda_3+\lambda_4\right)\right]=0\,. \tag{A.20c}$$

We use (A.20a) to remove m^2 from the remaining equations and obtain

$$\begin{aligned}\frac{v\varepsilon_1}{4\sqrt{2}}\left[-12M_S^2+v^2\left(-1+\varepsilon_1^2\right)\left(3\lambda_2-\lambda_3-\lambda_4\right)\right]&=0\,,\\ \frac{v\varepsilon_2}{4\sqrt{2}}\left[-12M_S^2+v^2\left(-1+\varepsilon_2^2\right)\left(3\lambda_2-\lambda_3-\lambda_4\right)\right]&=0\,.\end{aligned} \tag{A.21}$$

The solutions with nonzero $\varepsilon_{1,2}$ to the equations above are of the form

$$\varepsilon_1^2=\varepsilon_2^2=1-\Delta_+\ ,\ \ v^2=4\left(-\frac{m^2}{3\lambda_1+2\lambda_3+2\lambda_4}+\frac{2M_S^2}{-3\lambda_2+\lambda_3+\lambda_4}\right)\,. \tag{A.22}$$

Thus, we obtain a VEV configuration of the form $v/2\left(1,\pm\sqrt{1-\Delta_+},\pm\sqrt{1-\Delta_+}\right)$. This is the solution used in [56] with a different parametrization.